Received: 16 October 2023 | Accepted: 12 April 2024

DOI: 10.1111/mice.13216

COMPUTER-AIDED CIVIL AND INFRASTRUCTURE ENGINEERING WILEY

RESEARCH ARTICLE

Multistage charging facility planning on the expressway coordinated with the power structure transformation

Tian-yu Zhang[1] | **En-jian Yao**[1] | **Yang Yang**[1] | **Hong-Ming Yang**[2] | **Dong-bo Guo**[1] | **David Z. W. Wang**[3]

[1]Key Laboratory of Transport Industry of Big Data Application Technologies for Comprehensive Transport, Beijing Jiaotong University, Beijing, China

[2]Hunan Provincial Engineering Research Center of Electric Transportation and Smart Distributed Network, Hunan Provincial Key Laboratory of Smart Grids Operation and Control, School of Electrical Engineering and Information, Changsha University of Science and Technology, Changsha, China

[3]School of Civil and Environmental Engineering, Nanyang Technological University, Singapore, Singapore

Correspondence
En-jian Yao, Key Laboratory of Transport Industry of Big Data Application Technologies for Comprehensive Transport, Beijing Jiaotong University, Beijing, China.
Email: enjyao@bjtu.edu.cn

Funding information
National Key R&D Program of China, Grant/Award Number: 2023YFB4302703; National Natural Science Foundation of China, Grant/Award Numbers: 52172312, 71931003; Singapore Ministry of Education Academic Research Fund (AcRF) Tier 1 project, Grant/Award Number: RT22/22

Abstract

This study presents a novel multistage expressway fast charging station (EFCS) planning problem coordinated with the dynamic regional power structure (PS) transformation. Under the prerequisite of the EFCS network's sustainable operation, network accessibility, and orderly construction, a three-step planning method oriented to the enhancement of energy saving and emission reduction (ESER) benefits and rationalization of facility utilization is developed: (i) EV-expanded network, (ii) multiagent-based dynamic traffic assignment (MA-DTA), and (iii) deployment refinement. Embedding the MA-DTA and customized refinement strategy into the iterative planning structure enables the integration of operations and planning of the EFCS network. A numerical experiment and an empirical study in the Shandong Peninsula urban agglomeration are conducted. It demonstrates that the method can find a high-quality solution within acceptable computation time and is applicable to realistic large-scale EFCS planning. The planning method can effectively play the role of economy and facility in inducing EV users' charging demands, thus enhancing the overall ESER benefits. The integration of operation and planning is proven effective in reasonably matching the supply and demand of facility service and charging loads in a full-time period. Further, the multistage EFCS planning schemes during 2025–2045 are explored, and some insightful policy implications are revealed.

1 | INTRODUCTION

At present, driven by the policy of energy saving and emission reduction (ESER) in transportation and the promotion of social recognition, strong momentum is emerging in the electric vehicle (EV) markets. According to the "Global EV Market Outlook 2021", EVs worldwide increased by 41% in 2020 (Bibra et al., 2021). And, the intercity travel demand of EV users is growing with the increase in the driving range of EVs. In response, the government is paying increasing attention to constructing charging networks on expressways (IEA, 2023). By October

2022, a total of 16,721 charging stations have been built in 3974 of China's 6618 expressway service areas (The People's Republic of China, 2022). However, the existing network cannot effectively meet the growing demand for EV users' medium- to long-distance travel, as the mismatch between demand and supply of facilities is still prominent (Kang et al., 2022). As an energy supplementary infrastructure, a reasonable deployment of an expressway fast charging station (EFCS) network is an important basis for guaranteeing EVs' intercity travel, ensuring the operators' profitability, and achieving the goal of ESER on the expressway.

To promote EFCS network construction, the government expects to decarbonize power generation (PG) through energy structure transformation (Bogdanov et al., 2021). EVs can clean up the end-use of energy for transport, but their source of electricity has been much criticized. The power of most charging stations comes from thermal power (TP) plants (Rietmann et al., 2020). In the current Chinese power structure (PS), the whole life cycle CO_2 emission per 100 km of EVs is 19.01 kg, a 44.1% reduction compared to gasoline vehicles (GVs; Wang, Wang, et al., 2021). To realize the true "zero emissions," the government has developed a series of PS transformation paths to continuously reduce the proportion of fossil energy and gradually promote green power (GP) generation. However, influenced by natural resources and socioeconomics, it is inevitable that within a large network, there will be PS differences across regions and over time.

In addition, a mature network of EFCS is essential to accommodate more EV intercity travel in the future, but it is not built at one time. The EFCS deployment needs to dynamically adapt to growing market demand and the changing external environment in the multistage process (Xie & Lin, 2021). Among them, the market demand depends on vehicle ownership, EV percentage, and the battery degradation degree; the external environment refers to PS. By orderly construction and expansion of charging facilities in different stages, the charging network can provide charging services with a high level of service (LOS) while avoiding the waste of facility resources.

In summary, the multistage EFCS planning should balance the facility service and the charging load in both spatial and temporal dimensions. At the spatial dimension, the two roles of supply and inducement of the charging network need to be given adequate attention. The first is to provide a convenient and high LOS energy replenishment for EVs during the trip. The second is to use facility deployment to guide EV users' charging choices with the uneven regional PS. At the temporal dimension, the dynamic evolution of charging demand and PS are considered to realize orderly EFCS planning. The literature review will elaborate on the current theoretical gaps and motivations of this study.

1.1 | Literature review and motivations

1.1.1 | Deployment approaches

There has been rich research on charging facility deployment (CFD) in recent decades. The deployment approach can be divided into two categories: the optimization approach and the planning approach.

Most research adopts optimization approaches. Based on the model structure, it can be classified into single-level and bilevel optimization models. For single-level optimization models, charging demand is usually concentrated as node-based demand, which is estimated according to EV users' range anxiety (Hu et al., 2019), vehicle trajectory data (Yang et al., 2017), or operation data (Zeng et al., 2019). The limitations of these models are as follows: (1) the travel process of vehicles on the traffic network is ignored, making it hard to capture the en-route charging demand (Zhang, Yao, et al., 2023); (2) the queuing effect in stations is ignored. The facility's capacity is mostly estimated simply by the static number of dwell or charging (Wang et al., 2019). In the bilevel optimization model, the upper level determines the optimal CFD, and the lower level is the traffic assignment model to capture the flow-based demand (He et al., 2018; Zhang et al., 2018). The model's shortcomings are as follows: (1) The traffic assignment models focus on the flow transmission on the traffic network (Ghosh-Dastidar & Adeli, 2006; Zhang et al., 2022). They are not applicable to capturing EVs' en-route charging demands and simulating charging station operation. (2) Dynamic traffic assignment (DTA) would cause the bilevel model to be computationally intractable, and its solution accuracy and computation speed are difficult to be applied to real large-scale networks.

In this regard, some researchers adopt a multicriteria decision-making (MCDM) approach (Ju et al., 2019; Kaya et al., 2020), such as AHP and TOPSIS, to plan the CFD. The MCDM approach considers a comprehensive range of aspects, that is, energy, environment, economy, geography, and transportation, and incorporates experts' opinions in different fields. However, the method has a certain degree of subjectivity due to the strong influence of the experts' own knowledge structure, cognitive level, and emotions.

In recent years, the limitations of optimization and MCDM approaches have been more widely recognized. A few researchers adopted an iteration-based planning approach for the CFD problem. Morro-Mello et al. (2019) proposed a new methodology, which considers the criteria of multiple entities and simulates the EV's state of charge (SOC) and flow throughout the day. To minimize the CFD's scale while satisfying the connectivity and coverage constraints, Huang and Savkin (2020) proposed a two-phase approach. Considering the battery degradation, vehicle

heterogeneity, and three optimal objectives, Wang, Zhao, et al. (2021) planned the CFD with an iterative refinement strategy. The iteration-based planning approach retains the optimization model's concept of finding the optimal solution while incorporating the advantages of the planning model's factors of comprehensiveness and high solution efficiency.

Motivation 1: Subject to the limitations of the optimization and the MCDM approaches, a CFD planning approach that combines solution accuracy and practical implementation needs to be proposed. In addition, most research on the CFD problem separates operation from planning. This causes the EFCS to have difficulty providing a sustainable LOS in the obtained scheme (Zhao et al., 2021).

1.1.2 | Planning objectives

In the planning of CFD, the interests of different entities, such as facility operators, EV users, and the power, are mainly considered. As the main body of construction and operation of charging facilities, operators are concerned about the project's economy. Specifically, the objective functions include the minimization of investment cost (Uslu & Kaya, 2021), operating profits (Chen et al., 2017; Ma & Xie, 2021), facility service coverage (He et al., 2016), and captured traffic flow (Wei et al., 2017). For EV users, the CFD needs to guarantee the convenience and economy of their travels and minimize the impact of charging events on their travels. It is mainly formulated as the minimized travel cost (Bao & Xie, 2021; An et al., 2020), consisting of the charging cost, queuing time, detour time, and travel time. In addition, some researchers focus on the integration of transport networks with power systems. It is required to guarantee the power distribution network's investment economy, supply reliability, and power quality. The objective functions mainly include minimization of the infrastructure's investment cost (Hajibabai et al., 2023; Liu et al., 2023), power loss (Yang et al., 2020), voltage deviation (Amiri et al., 2018), and power expansion cost (Wang et al., 2018).

Motivation 2: The ESER benefits are mostly used as statistical rather than decision indicators in the CFD's planning. The maximization of ESER benefits is one of the essential driving forces for the government.

1.1.3 | Multistage planning

The multistage planning has been applied to various facility planning problems and is divided into two main categories based on model structures.

The first category is overall planning (Miralinaghi et al., 2017; Pourgholamali et al., 2023), in which the multistage deployments are optimized simultaneously to obtain the global optimum. However, constrained by the model structure, the factors considered in this class of models are limited and difficult to apply in realistic large-scale planning scenarios.

To solve this issue, some researchers use stage-by-stage planning, where the network deployment in each stage is carried out sequentially. The planning directions include forward (Li et al., 2022) and backward (Staricco et al., 2020; Zhang, Wang, et al., 2023). In the forward planning, the network is planned sequentially from the near stage to the future stage, and the facilities built in the earlier stage are forced to be used in the future. In contrast, the network is planned sequentially from the future to the near stage in the backward planning. The obtained station construction set in the future stage is the input as the station alternative set for the planning in the near stage. Comparing forward and backward planning, Yang et al. (2023) found that the facilities built in the early stage may be contrary to the last deployment, resulting in wasted or inefficient facility resources in forward planning. From a long-term perspective, the network deployments obtained by backward planning method are more economical and efficient.

Motivation 3: The above research provides an important foundation for solving the multistage CFD problem in realistic scenarios. The grasp of the external environment changes in different stages needs to be more comprehensive.

1.2 | Objectives and contributions

This study aims to achieve a multistage orderly planning of the EFCS in the dynamic regional PS transformation. With an orientation toward improving ESER benefits, a three-step planning method for EFCS multistage deployment is proposed. It consists of EV-expanded network, multiagent-based dynamic traffic assignment (MA-DTA), and deployment refinement. The expressway of the Shandong Peninsula urban agglomeration is selected as the empirical case. The substantial contributions are as follows.

New problem and new model: This study tries to plan the multistage EFCS network deployment coordinated with the dynamic regional PS transformation. The planning is oriented toward maximizing ESER benefits from vehicle electrification and PS transformation. The model is proposed based on the design concepts of the ESER, sustainable operation, network accessibility, and orderly

construction. Hence, its model structure is novel and complex.

Iterative planning method integrating the operation and planning: With the iterative planning structure, a three-step planning method is developed to solve the proposed multistage EFCS network deployment problem in a large-scale scenario. By embedding the improved MA-DTA and the customized refinement strategy into the iterative planning structure, the three-step planning method enables the integration of the operation and planning of the EFCS network. The results of the numerical experiment and an empirical study demonstrate that the method can efficiently get a high-quality solution within acceptable computational time and is applicable to realistic large-scale EFCS planning.

The remainder of this paper is arranged as follows. The problem description and a conceptual optimization model are established in Sections 2 and 3. The methodology is illustrated in Section 4. A numerical experiment and an empirical study are discussed in Sections 5 and 6. The findings are concluded in Section 7.

2 | PROBLEM DESCRIPTION

For the proposed EFCS multistage deployment problem, this study balances the facility's service and the charging load in both spatial and temporal dimensions.

2.1 | Spatial dimension

At the spatial level, the EFCS network's energy supply and demand inducement roles need to be given adequate attention.

2.1.1 | Energy supply

Accurately capturing EV users' multiple en-route charging demands is the foundation of a sustainable energy supply for EFCS networks.

Limited by the driving range, EV users will inevitably need to charge several times during the intercity travel. Figure 1 depicts the abstracted driving process of an EV with multiple en-route charging demands. Four SOC thresholds S_k^0, $S^{\exp}$, S^1, and S^2 are set considering the battery degradation, fast charging mode, EV users' second travel demands, and driving range anxiety, where S_k^0 denotes the fully charged SOC of EV group in stage k. As the EV market develops, the proportion of used batteries in the EV group will gradually increase until it tends to be within a stable range. In this study, the

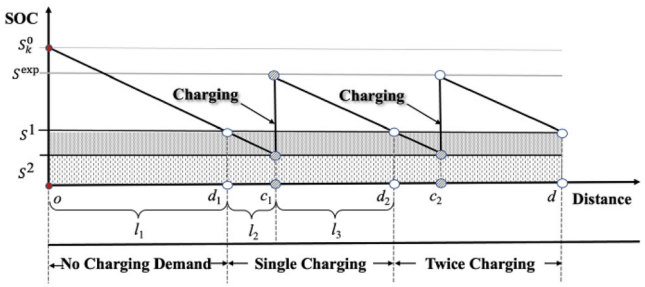

FIGURE 1 An electric vehicle (EV) with multiple en-route charging demands.

sampling approach is adopted to describe the battery degradation of the EV group at different stages. The effective battery capacity in stage k is assumed to follow a truncated normal distribution (Wang, Zhao, et al., 2021), $S_k^0 \sim \mathrm{Nor}(\mu_k, \sigma_k^2, a, b)$, where μ_k and σ_k^2 are the mean and standard deviation of battery effective capacity, and a and b are the upper and lower bounds. $S^{\exp}$ is the expected SOC of EV charge en-route. The fast charger operates in the constant-current/constant-voltage mode (Murnane & Ghazel, 2017). When the SOC is low, the fast charger operates in a constant-current mode and the SOC increases consistently from 20% S_k^0 to 80% S_k^0 in 30 min. If charging continues, the charger switches to a constant-voltage mode and it takes about 1.5 h to charge fully. Therefore, considering the charging time economy, $S^{\exp}$ is set at 80% of the current effective battery capacity S_k^0. S^1 is the minimum SOC when EV leaves the expressway, which guarantees the subsequent energy demands for travel within the city. S^2 is EV users' tolerance limit of SOC when driving.

2.1.2 | Demand inducement

In the region with uneven PS, planners should induce EV users to GP-rich areas for energy replenishment, thus improving the network's ESER benefits. The demand inducement roles of differentiated charging prices and facility allocation are depicted in Figure 2.

Figure 2a is an abstracted path for EV coming from (o, d). It passes through one toll station d_1, and two charging stations c_1 and c_2, where the powers come from GP and TP, respectively. It is assumed that the EV choosing path {o, d_1, c_1, c_2, d} needs to be charged at either station c_1 and c_2, and only once, to complete the trip. In Figure 2b, the C_1-axis and C_2-axis represent the generalized charging costs for c_1 and c_2. The costs consist of the energy replenishment cost and the waiting time cost. The N-axis represents the number of EVs that charge at c_1 and c_2 simultaneously. $C_1^{\min}$ and $C_2^{\min}$ denote the minimum generalized charging costs of c_1 and c_2, only including the energy replenishment cost.

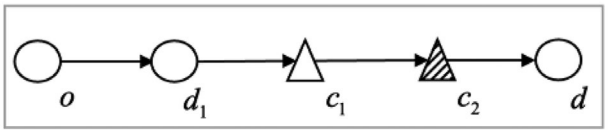

(a) Abstracted route for EV on expressway

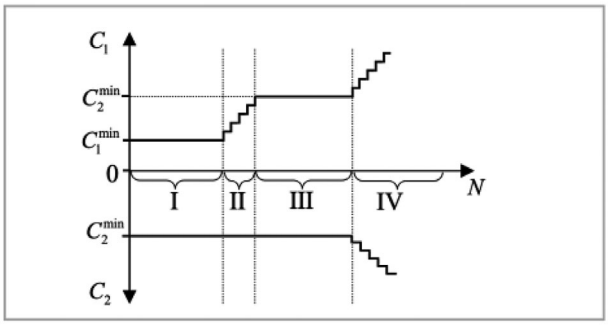

(b) Generalized charging cost of station

FIGURE 2 Abstracted charging demand inducement.

Assuming that the EVs charge the same amount at c_1 and c_2, and the power price of GP is set less than that of TP, then $C_1^{\min} < C_2^{\min}$.

Observing the growth curves of C_1 and C_2, it can be divided into four stages. In stage I, chargers are available in c_1, and its waiting time is 0. At this point, EV users charge at c_1. In stage II, queuing is generated in c_1 and C_1 gradually increases but remains less than $C_2^{\min}$ when EV users still charge at c_1. In stage III, EV users choose c_2 when $C_1 = C_2^{\min}$. In stage IV, a queue is generated in c_1 and c_2, and EV users alternately charge at c_1 and c_2.

Figure 2 illustrates how EV users can be induced to charge at the GP area, that is, expanding the length of stages I and II. The first method is economic induction. The length of stage II increases by enlarging the gap between $C_1^{\min}$ and $C_2^{\min}$. The second method is facility induction. The length of stage I can be increased by adjusting the allocation of facility resources in c_1 and c_2. The proposed model is designed based on the above two methods.

2.2 | Temporal dimension

In multistage EFCS deployments, it is essential to consider the scenario changes in various stages.

As time progressed, in addition to the change in vehicle ownership, EV percentage, and PS, the battery degradation of EV groups due to the increase in the number of old EVs cannot be ignored. The battery degradation of EVs is mainly caused by calendar and cycle aging. Calendar aging refers to the inherent degradation of the battery over time. Cycle aging refers to the maximum number of charge/discharge cycles before the battery fails. The battery capacity will degrade to varying degrees as time passes. Especially for EV users in intercity travel, the available battery capacity significantly affects their charging frequency, charging amount, charging location, and travel route.

3 | A CONCEPTUAL OPTIMIZATION MODEL

This section proposes a conceptual optimization model to demonstrate the mathematical formulation of the multistage EFCS deployment problem. The computational difficulties of applying the optimization model to solve the realistic large-scale EFCS deployment are discussed. It provides a better understanding of the proposed methodology in Section 4.

3.1 | A conceptual optimization model

This study considers EFCS performances from the perspectives of investors, EV users, and the government. For investors, the construction economics and sustainable operation are key factors. For EV users, they focus on the cost of traveling and replenishing energy. The government needs to guarantee the network accessibility of the EFCS network and care about its ESER benefits. A generalized optimization model considering the above factors is proposed as follows.

$$\begin{cases} \mathrm{Min}_{x_{i,k}(\mathfrak{R}),y_{i,k}(\mathfrak{R})} f_{\mathrm{ConstructionCost}}(N,\mathfrak{R},E) \\ \mathrm{Min}_{P_{k,m*}(\mathfrak{R})} f_{\mathrm{TravelCost}}(\mathrm{MA}-\mathrm{DTA}(P_{k,m*}(\mathfrak{R}),N,\mathfrak{R},E)) \\ \mathrm{Max}_{x_{i,k}(\mathfrak{R}),y_{i,k}(\mathfrak{R}),P_{k,m*}(\mathfrak{R})} f_{\mathrm{ESER}}(\mathrm{MA}-\mathrm{DTA}(P_{k,m*}(\mathfrak{R}),N,\mathfrak{R},E)) \end{cases} \quad (1)$$

s.t.

$$\beta^{z,down} \le U_{k,i}(\mathfrak{R}) \le \beta^{z,up} \forall i \in I_k^z(\mathfrak{R}), z \in Z, k \in K \quad (2)$$

$$L_{k,o,d}^e(N,\mathfrak{R}) \notin \emptyset \forall o \in O, d \in D, k \in K \quad (3)$$

$$x_{i,k}(\mathfrak{R}) \in \begin{cases} \{0,1\} \forall i \in I, k == k^{\max} \\ \{0,1\} \forall i \in X''_{k+1}, k \in \{1,2,\dots,k^{\max}-1\} \\ \{0\} \forall i \notin X''_{k+1}, k \in \{1,2,\dots,k^{\max}-1\} \end{cases} \quad (4)$$

$$y_{i,k}(\mathfrak{R}) \in \begin{Bmatrix} [y^{\min} \cdot x_{i,k}(\mathfrak{R}), \infty], \forall i \in I, k == k^{\max} \\ [y^{\min} \cdot x_{i,k}(\mathfrak{R}), y''_{i,k+1} \cdot x_{i,k}(\mathfrak{R})], \\ \forall i \in X''_{k+1}, k \in \{1,2,\dots,k^{\max}-1\} \\ \{0\}, \forall i \notin X''_{k+1}, k \in \{1,2,\dots,k^{\max}-1\} \end{Bmatrix} \quad (5)$$

In this study, O and D are the sets of origin and destination (OD), $o \in O$, $d \in D$. I is the set of service areas, $i \in I$. M is the set of vehicle types, $m \in M = \{h, e\}$, where h refers to GV and e refers to EV. Z is the set of power types, $z \in Z = \{g, f\}$. It includes TP f and GP g, where the raw materials are represented by coal and nuclear, respectively. To simplify the problem, the electricity of any station is supplied by only one type of power. K denotes the set of planning stages, $k \in K = \{1, 2, \ldots, k^{\max}\}$. $\mathfrak{R}$, N, and E are the charging, expressway, and power distribution networks, respectively. The optimal deployment scheme of charging stations and chargers in stage k is denoted as X''_k, Y''_k. $U_{k,i}(\mathfrak{R})$ is the facility utilization, which refers to the average value of status of charging station i under $\mathfrak{R}$ layout for a whole day in stage k. $\beta^{z,up}$ and $\beta^{z,down}$ are the upper and lower bounds of facility utilization in power z. $I^z_k(\mathfrak{R})$ is the set of charging stations in power z under $\mathfrak{R}$ layout in stage k. $L^e_{k,o,d}(N, \mathfrak{R})$ is the effective route sets of EVs between (o, d) on the network of $(N, \mathfrak{R})$ in stage k. y^{min} is the minimum number of chargers for a single charging station. The notation of sets, parameters, and variables are listed in the Appendix.

As shown in Equation (1), this model contains three optimization objectives. The first objective function is to minimize the construction cost of the charging network. It depends on $x_{i,k}(\mathfrak{R})$ and $y_{i,k}(\mathfrak{R})$, where $x_{i,k}(\mathfrak{R})$ is the binary varible to judge whether a charging station is built at service area i under $\mathfrak{R}$ layout in stage k. If it is, then $x_{i,k}(\mathfrak{R}) = 1$, otherwise $x_{i,k}(\mathfrak{R}) = 0$. And $y_{i,k}(\mathfrak{R})$ is the corresponding number of chargers. $y''_{i,k+1}$ is the optimal capacity of the station i in stage k+1. The second one is to minimize the travel costs of EV users. The decision variable $P_{k,m*}(\mathfrak{R})$ is the choosing probability of path l for m^*, which decides the EV users' travel and charging process. m^* is an abbreviation for $m^* = {}^m_{o,d,t,l}$, which means the vehicle of type m that departs at time t and chooses path l through (o, d). As for the third one, it maximizes the network's ESER benefits that interest the government. The travel cost and ESER benefits are calculated by the MA-DTA model, which simulates the traffic flow transmission and charging network's operation dynamically.

Meanwhile, to guarantee sustainable operation and construction economy, the constraints of facility utilization in different power regions are proposed, as illustrated in Equation (2). Equation (3) formulates the relationship between the effective route set $L^e_{k,o,d}(N, \mathfrak{R})$ and the empty set $\emptyset$. It guarantees the network accessibility, referring to whether EVs can achieve intercity travel between any OD pair under extreme conditions (with a tolerable SOC limitation, where $S^{\exp} = S^0_k$, $S^1 = 0$, and $S^2 = 0$). Equations (4) and (5) present the backward construction constraints for the charging station's location and capacity.

3.2 | Challenges and application intractability

Solutions to complex multiobjective optimization problems mostly use heuristic algorithms to obtain the Pareto frontier. However, due to the following three intractable challenges, extending to the large-scale network in real world is technically impossible.

First, the model involves a wide variety of variables due to its concept of integrating operation and planning. At the planning level, the decision variables are the charging station's location and capacity. At the operation level, it involves EV users' travel and charging decisions, and the real-time status of EVs, road networks, and charging networks. Second, the large-scale expressway and massive traffic flow will lead to many variables in the realistic planning scenario. For example, an expressway has 40 service areas, 100,000 vehicles per day, and 20% EV penetration. The minimum and maximum charger thresholds are assumed to be 4 and 20, respectively. It is estimated that there is over $40 \times (20 - 4) \times (100000 \times 20\%) = 12.8$ million decision variables. And the number of real-time status variables in the system is far beyond this order of magnitude. Third, the multistage overall planning leads to exponential growth in the number of variables, resulting in an explosion in solution time.

Due to the above issues, obtaining a reasonable solution in an acceptable time is difficult, even for heuristic algorithms (Akhand et al., 2020). Therefore, some decomposition techniques, such as operation decomposition and iterative or stepwise methods, are necessary to make the model solvable. However, the following modeling challenges hinder the application of operation decomposition. Due to the heterogeneity of EVs (caused by OD, departure time, travel path, and battery health), the en-route charging demand varies in terms of time, location, and charging amount, making it challenging to estimate EVs' dynamic demand through the mathematical modeling. Generally, the charging service is simplified to the mathematical queuing models, such as the D/D/S system. It requires deterministic arrival and service rates, which is challenging to derive continuous closed-form functions for the service process with differentiated charging demands. In contrast, the structure of the iterative or stepwise planning method is made up of multiple submodules connected by mathematical logic relationships. The submodules may be in various forms, such as mathematical optimization models, logical judgment models, data-driven or multi-agent-based simulation models, and so forth. The structure allows for more factors to be considered in their iterations or steps, such as the charging station operation in this problem.

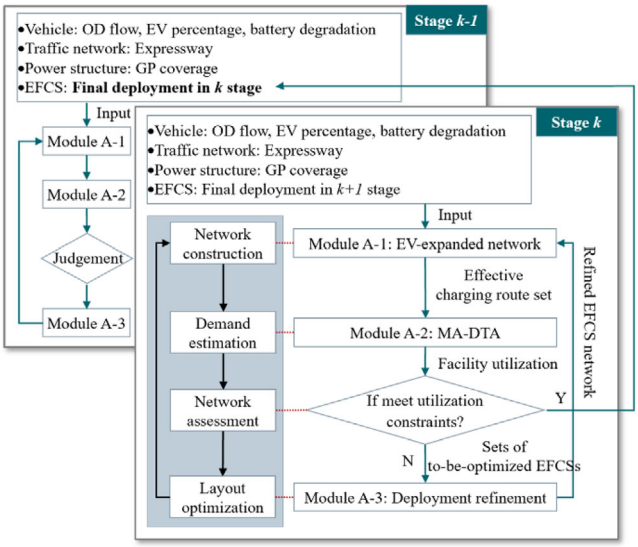

FIGURE 3 Framework of the proposed method.

Based on the above discussion, working to solve the large-scale multistage EFCS deployment problem, an iterative-based planning method is proposed.

4 | METHODOLOGY

This section proposes a three-step planning method for solving the large-scale multistage EFCS deployment problem, based on the design thought "Network construction → Demand estimation → Network assessment → Deployment optimization." Figure 3 presents the framework of the proposed method under the planning stage k.

The model inputs OD flow, traffic network, GP coverage in stage k, expressway, and the obtained final EFCS deployment in stage k+1. Based on the expressway and charging network, Model A-1 builds the effective charging route sets, considering EV users' multiple en-route charging demands. To realize the "Demand estimation," an MA-DTA model is proposed in Model A-2 to estimate EV users' dynamic charging demand responses and simulate the traffic flow transmission and the charging station operation dynamically. In the "Network assessment" phase, the judgment module gets the sets of to-be-optimized EFCSs based on the facility utilization outputted from Model A-2 and passes them to Model A-3. These charging stations' locations and capacities are refined with the guidance of improving ESER benefits and rationalizing facility utilization. Further, the refined EFCS deployment is returned to Model A-1. The iteration ends when all stations' utilizations are within a reasonable range. Finally, the final deployment in stage k is outputted into the model in stage $k-1$ so that the charging network is planned stage by stage inversely.

Next, the modeling and functions of each submodule are described in detail.

4.1 | Module A-1: EV-expanded network

In Module A-1, the effective travel route sets for GV and EV are developed to provide the data basis for the next step. Based on the current expressway, the EFCS deployment, and the above four SOC thresholds, the GV and EV route search algorithms are constructed, and modulated as the nonlinear functions, that is, $L^{h}_{o,d}(N) = f^{h}(N, \Omega)$ and $L^{e}_{o,d}(N, \mathfrak{R}) = f^{e}(S^0, S^{\exp}, S^1, S^2, L^{h}_{o,d}(N), \mathfrak{R}, n)$. The specific procedure is elaborated below:

Step 1: *Construction of base route sets*. According to the topology of the expressway, the Dijkstra algorithm and the improved Depth-First algorithm are used to get the set of shortest routes $L^{shortest}_{o,d}(N)$ and all routes $L^{all}_{o,d}(N)$ in turn.

Step 2: *Construction of GV effective route set* $L^{h}_{o,d}(N)$. Based on $L^{shortest}_{o,d}(N)$ and $L^{all}_{o,d}(N)$, the amplification factor Ω is introduced, and the routes with lengths less than $\Omega \cdot L^{shortest}_{o,d}(N)$ are regarded as the effective route set for GVs.

Step 3: *Construction of EV effective route set* $L^{e}_{k,o,d}(N, \mathfrak{R})$.

Step 3.1: *Setting the maximum times of en-route charging n*. According to the topology of the expressway and the driving range of EVs, the maximum times of en-route charging n is preset. At this time, EV users can charge 0, 1,…, n times during the trip.

Step 3.2: *Construction of EV charging route alternative set*. First, based on the GV effective route set $L^{h}_{o,d}(N)$ and the EFCS deployment $\mathfrak{R}$, the sets of EV travel routes and charging routes are obtained. For example, a GV travel route is represented as $\{o, d_1, d_2, \ldots, d_x, d\}$, where $o, d_1, \ldots, d_x$ are the toll stations passed on the way. The EV travel route $\{o, d_1, c_1, \ldots, c_i, \ldots, c_n, d_x, d\}$ is obtained by adding the charging stations $\{c_1, \ldots, c_i, \ldots, c_n\}$ passed on the GV route. $\{o, c_1, \ldots, c_i, \ldots, c_n, d\}$ is the charging route, combined by the OD and the charging stations passed on the GV route. Then, according to the order list of the charging stations and the maximum times of en-route charging n, a total of $\sum_{i=0}^{\min(n,m)} C^{i}_{m}$ EV charging route alternative sets are formed by permutation.

Step 3.3: *Judgment of charging route effectiveness*. According to the description in Section 2.1.1, the charging route $\{o, c_1, \ldots, c_i, \ldots, c_n, d\}$ needs to satisfy

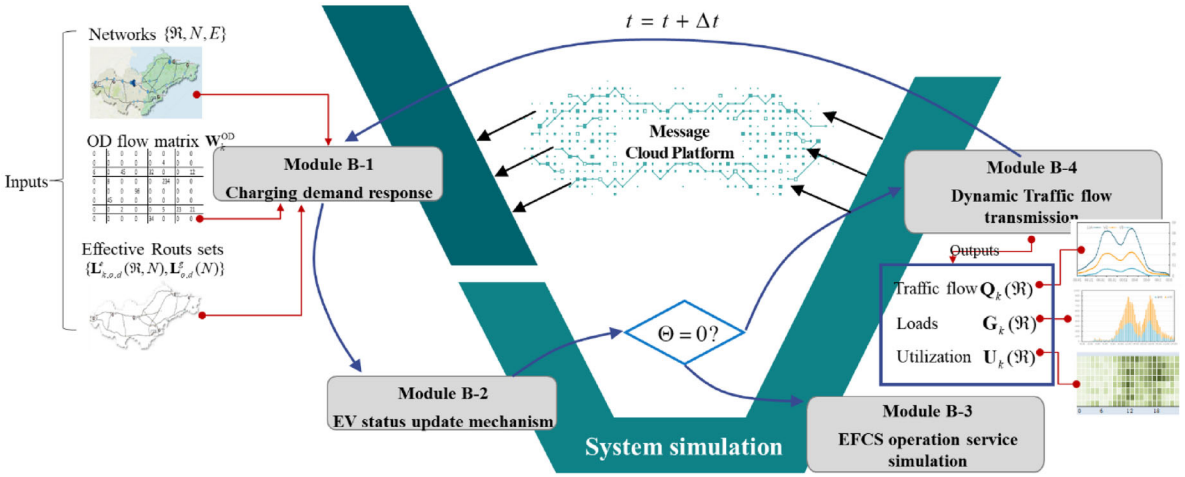

FIGURE 4 Framework of the proposed multiagent-based dynamic traffic assignment (MA-DTA).

the following three distance constraints: (1) Considering S_k^0 and S^1, the distance from the origin to the first charging station needs to satisfy $\Delta d(o, d_1) \le l_1$; (2) considering $S^{\exp}$ and S^2, the distance between any two consecutive passing charging stations on the way needs to satisfy $\Delta d(c_i, c_{i+1}) \le l_2 + l_3$; (3) considering $S^{\exp}$ and S^1, the distance from the last charging station to the destination needs to satisfy $\Delta d(c_n, d) \le l_3$. Only the routes that satisfy the above conditions can be regarded as effective charging routes for EVs.

4.2 | Module A-2: MA-DTA

In Module A-2, the real-time status of expressways, charging networks, and mixed traffic flows are monitored accurately and comprehensively, which is essential to assess the EFCS deployment and to find the optimization direction. The MA-DTA model consists of two layers, that is, the agent decision layer (Module B-1: Charging demand response) and the system simulation layer (Module B-2: EV status update mechanism; Module B-3: EFCS operation service simulation; Module B-4: Dynamic traffic flow transmission). Figure 4 shows the interaction among the modules.

In MA-DTA, the charging demand response of agents is presented in Module B-1. The agent's travel route determining the locations of en-route charging is chosen at the departure time based on the path size logit (PSL) model. In the system simulation layer, the system's full-day operation of vehicles, chargers, and networks is simulated. Specifically, the charging station operation service (Model B-3) for EVs in the charging status and the dynamic traffic flow transmission (Model B-4) for EVs in the driving status are performed according to the real-time status update of EVs (Model B-2), respectively. At the end of each period, multiple entities of information in the system, including vehicles, chargers, and roads, are uploaded to the Message Cloud Platform in real time. Then, the information is synchronized to EVs via mobile communication devices to provide accurate, real-time, and multiple information for their charging route decisions.

To represent the functional positioning of MA-DTA model in the proposed three-step planning method, it is formulated as a nonlinear and highly nonconvex function, $\Xi_{\text{MAS-DSUE}}(\cdot)$, with a simplified input and output form as follows.

$$[\mathbf{Q}_k(\mathfrak{R}), \mathbf{G}_k(\mathfrak{R}), \mathbf{U}_k(\mathfrak{R})] = \Xi_{\text{MAS-DSUE}} \begin{bmatrix} \mathfrak{R}, N, E, \mathbf{L}^e_{k,o,d}(\mathfrak{R}, N), \\ \mathbf{L}^g_{o,d}(N), \mathbf{W}^{\text{OD}}_k \end{bmatrix} \tag{6}$$

where $\mathbf{W}_k^{\text{OD}}$ is the OD travel matrix in stage k. Through the simulation, three three-dimensional spatial–temporal-status matrices, $\mathbf{Q}_k(\mathfrak{R})$, $\mathbf{G}_k(\mathfrak{R})$, and $\mathbf{U}_k(\mathfrak{R})$, which represent the traffic flow, charging load, and facility utilization under the charging network $\mathfrak{R}$ in stage k, are output. And, $\mathbf{U}_k(\mathfrak{R})$ is the key decision indicator for facility deployment refinement in Module A-3.

(1) Module B-1: Charging demand response

At the departure time, EV users must decide which route to travel, whether to charge and where to charge, that is, the charging route. Relying on the Message Cloud Platform, users can master complete real-time traffic network information (i.e., congestion and estimated travel time of each road section) and charging network information (i.e., queue length and estimated minimum queue time of each charging station) at the departure time.

Following Wardrop's first principle, all users choose the route with the lowest travel cost estimated by themselves. Eventually, the traffic network reaches stochastic dynamic user equilibrium (SDUE) status, which is represented as follows:

$$\begin{aligned}&\text{Min } Z_k^{\text{tra}}(\mathfrak{R})\\&=\sum_{t\in T}\sum_{o\in O}\sum_{d\in D}\sum_{m\in\{e,h\}}\sum_{l\in K_{rs}^m(\mathfrak{R})} C_{k,m*}(\mathfrak{R})\cdot q_{k,o,d}^{m,t}\cdot P_{k,m*}(\mathfrak{R})\end{aligned} \tag{7}$$

$$C_{k,m*}(\mathfrak{R})=\begin{cases}\sum_{a\in A_l}\alpha\cdot\tau_{a,t}^{e}+\\ \sum_{c_i\in C_l}\left[\sum_{j\in\{g,f\}}\mu^j\cdot\gamma_{c_i}\cdot H_{k,c_i}^{e*}(\mathfrak{R})\right]\\ \quad+(t_{wk,c_i}^{e*}(\mathfrak{R})+t_{ck,c_i}^{e*}(\mathfrak{R}))\cdot\alpha\end{cases},m=e$$
$$\sum_{a\in A_l}(\alpha\cdot\tau_{a,t}^{h}+\mu^h\cdot H_{a,t}^{h}),m=h \tag{8}$$

$$P_{k,m*}(\mathfrak{R})=\frac{\exp[-\theta\cdot C_{k,m*}(\mathfrak{R})+\ln(M_{o,d,l}^m)]}{\sum_{l\in L_{o,d}^m(N,\mathfrak{R})}\exp[-\theta\cdot C_{k,m*}(\mathfrak{R})+\ln(M_{o,d,l}^m)]}$$
$$\forall o\in O,d\in D,l\in L_{o,d}^m(N,\mathfrak{R}),t\in T,m\in\{e,h\} \tag{9}$$

$$M_{o,d,l}^m=\sum_{a\in A_l}\left(\frac{\Delta l_a}{\Delta l_l}\cdot\frac{1}{\sum_{l\in L_{o,d}^m(N,\mathfrak{R})}\partial_{a,l}}\right) \tag{10}$$

$$H_a^{m,t}=\begin{cases}(1.359/\overline{v}_{a,t}-0.003\overline{v}_{a,t}\\ \quad+2.981\times10^{-5}\overline{v}_{a,t}^2+0.218)\cdot l_a, & m=e\\ (125.015/\overline{v}_{a,t}-0.097\overline{v}_{a,t}\\ \quad+9.220\times10^{-4}\overline{v}_{a,t}^2+7.056)\cdot l_a, & m=h\end{cases} \tag{11}$$

where $Z_k^{\text{tra}}(\mathfrak{R})$ is the total travel cost of vehicles under the charging network $\mathfrak{R}$ in stage k. $C_{k,m*}(\mathfrak{R})$ is the travel cost of $m*$. $q_{k,o,d}^{m,t}$ is the new flow between (o, d) at time t. α is the value of time. μ^g, μ^f, and μ^h are the energy prices of GP, TP, and gasoline, respectively. γ_{c_i} indicates the type of power supply for station i. $H_{a,t}^h$ is the energy consumption of GVs on road a at time t. $H_{c_i}^{e*}$ is the charging demand of $e*$ at station i. $t_{wk,c_i}^{e*}(\mathfrak{R})$ and $t_{ck,c_i}^{e*}(\mathfrak{R})$ are the queuing time and charging time of $e*$ at station i. θ is the discrete coefficient reflecting users' perception difference. $M_{o,d,l}^m$ is the correction term of path l through (o, d) for the vehicle of type m. l_a and l_l are the lengths of road a, and path l. $\partial_{a,l}$ is a binary variable, where $\partial_{a,l}=1$ means that road a is part of path l, otherwise $\partial_{a,l}=0$.

As shown in Equation (7), the MA-DTA objective is to minimize the total travel cost of both GVs and EVs. Equation (8) illustrates the components of GV and EV travel costs. Specifically, EVs' travel cost consists of the cost of travel time $\sum_{a\in A_l}\alpha\cdot\tau_{a,t}^{e}$, the cost of electricity consumption $\sum_{c_i\in C_l}\sum_{j\in\{g,f\}}\beta^j\cdot\gamma_{c_i}\cdot H_{k,c_i}^{e*}(\mathfrak{R})$, and the cost of queuing and charging time $\sum_{c_i\in C_l}(t_{wk,c_i}^{e*}(\mathfrak{R})+t_{ck,c_i}^{e*}(\mathfrak{R}))\cdot\alpha$. The GVs' travel cost consists of the cost of travel time $\sum_{a\in A_l}\alpha\cdot\tau_{a,t}^{h}$, and the cost of gasoline consumption $\sum_{a\in A_l}\beta^h\cdot H_{a,t}^h$. Equations (9) and (10) calculate the route-choosing probability. Referring to the mesoscopic fuel consumption model (Yao & Song, 2013), the energy consumptions of GV and EV are calculated by Equation (11).

(2) Module B-2:EV status update mechanism

In MA-DTA, each EV is tagged with two kinds of information. The first is static information, that is, origin, destination, travel route, charging route, and battery health status. The second one is dynamic information that changes with time, including real-time SOC, location, working status of EV Θ, and remaining time to end the current status.

There are two types of working status of EV: driving status $\Theta=1$ and charging status $\Theta=0$. The charging status refers to the process after the EV enters the charging station, including queuing and charging. The simulation system uses the sliding time window algorithm to calculate and update the remaining time for the EV to end its status. It can be divided into the remaining time to leave the current road and the current charging station. The paradigm of the time window movement on the simulation time horizon is explicitly described in Amiri et al. (2018). When the updated Θ turns from 1 to 0, EVs move from the expressway to the charging station to receive the charging service, and the specific process is described in Module B-3. When the updated Θ turns from 0 to 1, EVs leave the charging station and continue to drive on the expressway, and the specific process is described in Module B-4.

(3) Module B-3:EFCS operation service simulation

In Module B-3, the EFCS operation service offered to EVs with discrete arrivals and heterogeneity of charging volume is simulated. For charging stations, the static attributes include location, capacity, and power types; the dynamic attribute is the remaining operating time of each charger.

For the arriving EV, its status is switched from 1 to 0 and the charger with the minimum remaining operating time is selected for queuing and charging. As shown in

Equation (12), the end time of the EV charging status, that is, the working end time of the selected charger, is determined by the queuing time and the battery charging time. As shown in Equation (13), the queuing time is equal to the minimum remaining operating time of all chargers in the charging station at the current time. As shown in Equation (14), the charging time is calculated based on J. A. Mas' acceptable current law (Mas et al., 1972).

$$t^{e*}_{lk,c_i}(\mathfrak{R}) = t^{e*}_{ak,c_i}(\mathfrak{R}) + t^{e*}_{wk,c_i}(\mathfrak{R}) + t^{e*}_{ck,c_i}(\mathfrak{R}) \tag{12}$$

$$t^{e*}_{wk,c_i}(\mathfrak{R}) = \max\left\{0, \min_{p\in P_i}\left\{t^{\text{pile}}_{k,c_i,p,t}(\mathfrak{R})\right\} - t^{e*}_{\text{ak},c_i}(\mathfrak{R})\right\} \tag{13}$$

$$t^{e*}_{ck,c_i}(\mathfrak{R}) = 50\ln\left[(S^{\exp} - S^{e*}_{k,c_i}(\mathfrak{R}))/0.9371 + 1\right] \tag{14}$$

where $t^{\text{pile}}_{k,c_i,p,t}(\mathfrak{R})$ is the working end time of charger p at charging station i at time t under the charging network $\mathfrak{R}$ in stage k. $t^{e*}_{ak,c_i}(\mathfrak{R})$, $t^{e*}_{lk,c_i}(\mathfrak{R})$, $t^{e*}_{wk,c_i}(\mathfrak{R})$, and $t^{e*}_{ck,c_i}(\mathfrak{R})$ are the time of arrival, departure, waiting, and charging of e^* at charging station i under the charging network $\mathfrak{R}$ in stage k, respectively. $S^{e*}_{k,c_i}(\mathfrak{R})$ is the SOC of e^* when it arrives at charging station i under the charging network $\mathfrak{R}$ in stage k.

(4) Module B-4:Dynamic traffic flow transmission

In Module B-4, the transmission process of traffic flow on the expressway is simulated based on the dynamic traffic flow transmission model. Vehicles follow the first-in first-out principle in the transmission process. Traffic congestion on roads is estimated by the point queueing model. It should be noted that since the charging stations are relatively isolated from the expressway and connected via ramps, EVs receiving charging services are not considered as traffic loads. Specific descriptions of the DTA model are ignored here due to the limited space. After the simulation period, the updated road network information is delivered to the Message Cloud Platform, including the road's traffic load and travel time. Applying the method of successive averages, which efficiently solves the SDUE model, to the above simulation environment enables a fast solution of MA-DTA.

Finally, to demonstrate the applicability of the proposed "Dynamic" characteristics of MA-DTA in EVs en-route charging services, Table 1 details the differences among the MA-DTA, traditional DTA, and queuing theory.

4.3 | Module A-3: Refinement strategy

Based on the dynamic simulation from Module A-2, the daily statuses of multiagents, including EVs and chargers, are aggregated for the network assessment. Then, the EFCS network is refined to improve the ESER benefits and rationalize facility utilizations.

4.3.1 | Network assessment

The assessment indicators can be divided into two main categories: LOS and ESER benefits.

Charging network service

The LOS of the charging network is the primary concern for EV users. The average waiting and charging times are obtained based on the aggregation of Equations (13) and (14). The facility utilization $U_{k,i}(\mathfrak{R})$ is calculated by Equation (15). It reflects the dynamic level of supply and demand of charging stations.

$$U_{k,i}(\mathfrak{R}) = \sum_{t\in T}[q_{k,c_i,t}(\mathfrak{R})/y_{k,i}(\mathfrak{R})]/S' \tag{15}$$

where S' is the number of time parts. $q_{k,c_i,t}(\mathfrak{R})/y_{k,i}(\mathfrak{R})$ denotes the ratio of the number of vehicles at charging station i to the number of chargers at time t, that is, the average occupancy rate of chargers at the end of each time step. When $q_{k,c_i,t}(\mathfrak{R})/y_{k,i}(\mathfrak{R}) = 1$, it means that all chargers are working, and all EVs are charging. The higher the $U_{k,i}(\mathfrak{R})$, the greater the workload of station i is.

ESER benefits

The government values the ESER benefits brought by vehicle electrification and PS transformation. Therefore, three indicators, including standard coal (SC) savings, CO_2 emission reduction (CER), and GP percentage, are proposed.

SC savings. SC savings refers to the reduced total SC by PG. Considering the loss of EVs due to excessive queuing time, only the charging requests of EVs with a queuing time less than ψ are seen as the completed charging service. The effective electricity consumptions of TP and GP are calculated by Equation (16).

$$E^{\text{actual,z}}_{k}(\mathfrak{R}) = \{E^{z}_{k}(\mathfrak{R}) | t^{e*}_{wk,c_i}(\mathfrak{R}) \le \psi\} \forall z \in Z \tag{16}$$

where $E^{\text{actual,z}}_{k}(\mathfrak{R})$ and $E^{z}_{k}(\mathfrak{R})$ are the actual PG and all charging demands in the region with power z.

Then, the actual power origin from TP and GP are converted into the SC to calculate the energy saving, shown as

TABLE 1 The function list of multiagent-based dynamic traffic assignment (MA-DTA), dynamic traffic assignment (DTA), and queuing theory.

"Dynamic" characteristic	Function lists		
	Traditional DTA	**Queuing theory**	**Proposed MA-DTA**
Demand	• Dynamic traffic flow	• Deterministic arrival rate of electric vehicles (EVs)	• Dynamic traffic flow • Discrete charging loads
Transmission	• Dynamic traffic flow transmission	• Deterministic service rate of charging station	• Dynamic traffic flow transmission • Dynamic operation service of charging stations • Differentiated charging service
Impedance	• Real-time impedance of the traffic network	• Preset the queuing time of free flow	• Real-time impedance of the traffic network • Real-time operational status of the charging network

follows.

$$ENG_k^z(\mathfrak{R}) = E_k^{\text{actual,z}}(\mathfrak{R}) \cdot \xi^{\text{e}} \forall z \in Z \tag{17}$$

where $ENG_k^z(\mathfrak{R})$ is the quantity of SC required to supply the equivalent energy in the region with power z. ξ^{e} is the SC coefficient of power.

CO_2 emission reduction. To assess the environmental benefits, two indicators, are proposed in Equations (17) and (18). $CER_k^{PG}(\mathfrak{R})$ refers to the CER by vehicle electrification, which is the CO_2 saved by converting gasoline into electricity under the equivalent driving mileage. And $CER_k^{PST}(\mathfrak{R})$ refers to the CER by PS transformation, which is calculated by replacing TP with GP while supplying the equivalent energy.

$$CER_k^{PG}(\mathfrak{R}) = \sum_{z \in Z} E_k^{\text{acutal,z}}(\mathfrak{R}) \cdot (\lambda^{\text{gas}} - \lambda^{f}) \tag{18}$$

$$CER_k^{PST}(\mathfrak{R}) = E_k^{\text{acutal,g}}(\mathfrak{R}) \cdot (\lambda^{\text{f}} - \lambda^{\text{g}}) \tag{19}$$

where λ^{gas}, λ^{f}, and λ^{g} are the carbon emission factors of gasoline, TP and GP, respectively.

Percentage of GP. The GP percentage refers to the GP generation to the total PG. Then, the actual GP percentage and the standardized GP percentage are calculated as follows.

$$P_k^{\text{actual,g}}(\mathfrak{R}) = E_k^{\text{actual,g}}(\mathfrak{R}) / [E_k^{\text{actual,g}}(\mathfrak{R}) + E_k^{\text{actual,f}}(\mathfrak{R})] \tag{20}$$

$$P_k^{\text{sta,g}}(\mathfrak{R}) = E_k^{\text{actual,g}}(\mathfrak{R}) / [E_k^{\text{g}}(\mathfrak{R}) + E_k^{f}(\mathfrak{R})] \tag{21}$$

where $P_k^{\text{actual,g}}(\mathfrak{R})$ denotes the actual GP percentage in the network considering the EV loss. However, due to different denominators, it is difficult to compare the GP percentage under different EFCS deployments horizontally. Therefore, a standard GP percentage $P_k^{\text{sta,g}}(\mathfrak{R})$, representing the proportion of effective PG of GP to the total power demand in the network, is proposed. It should be noted that when the network LOS reaches a sufficiently high level, that is, all EVs' queuing time are less than ψ, the values of $P_k^{\text{actual,g}}(\mathfrak{R})$ and $P_k^{\text{sta,g}}(\mathfrak{R})$ are equal.

4.3.2 | Deployment refinement

The refinement strategy is designed to improve the ESER benefits and the rationality of facility utilization for the EFCS network while safeguarding its network accessibility and orderly construction. Based on the greedy strategy, the locally optimal deployment refinement is made at each iteration with the hope of finding the global optimum in each planning stage.

Its pseudo-code is shown in Table 2. First, the to-be-optimized charging station and its optimization direction are found according to the facility's working status (line 1). Based on Equation (2), the four to-be-optimized sets of charging stations $G_k^{g,ex}(\mathfrak{R})$, $G_k^{f,ex}(\mathfrak{R})$, $G_k^{g,un}(\mathfrak{R})$, and $G_k^{f,un}(\mathfrak{R})$ are constructed. They denote the charging station sets with facility utilization above and below the threshold in the GP region and TP region, respectively.

Next, a backward elimination method is used to refine the to-be-optimized stations in the network to avoid high load and eliminate facility redundancy.

On the one hand, when the utilization exceeds the upper threshold, it indicates that the station has a high load. It is challenging to maintain a stable and reasonable LOS throughout the day. The refinement strategy is to increase the number of chargers by one unit in each iteration (lines 2–8) for all stations in $G_k^{g,ex}(\mathfrak{R})$ or $G_k^{f,ex}(\mathfrak{R})$. The refinement strategy sets a differentiated deployment refinement priority to tap the network's ESER benefits brought by PS transformation. It prioritizes the

TABLE 2 The pseudo-code of refinement strategy.

Pseudocode of the refinement algorithm
Input: $U_k(\mathfrak{R})$, $\beta^{z,up}$, $\beta^{z,down}$, y^{min}, $X_k(\mathfrak{R})$, $Y_k(\mathfrak{R})$, X^*_{k+1}, Y^*_{k+1}
Output: $X_k(\mathfrak{R}')$, $Y_k(\mathfrak{R}')$
1: Construct sets $G_k^{g,ex}(\mathfrak{R})$, $G_k^{f,ex}(\mathfrak{R})$, $G_k^{g,un}(\mathfrak{R})$, $G_k^{f,un}(\mathfrak{R})$
2: j←g
3: if $G_k^{g,ex}(\mathfrak{R}) \cup G_k^{g,un}(\mathfrak{R}) = \emptyset$ then
4: j←f
5: end if
6: for $i \in G_k^{j,ex}(\mathfrak{R})$ do
7: $y_{i,k}(\mathfrak{R}')$←$y_{i,k}(\mathfrak{R}) + 1$
8: end for
9: for $i \in G_k^{g,un}(\mathfrak{R}) \cup G_k^{f,un}(\mathfrak{R})$ do
10: if $y_{i,k}(\mathfrak{R}) - 1 < y^{min}$ do
11: delete station i
12: if Equation (3) ease to hold then
13: $x_{i,k}(\mathfrak{R}')$←0, $y_{i,k}(\mathfrak{R}')$←0
14: end if
15: else
16: $y_{i,k}(\mathfrak{R}')$←$y_{i,k}(\mathfrak{R}) - 1$
17: end if
18: end for

enhancement of the service capacity of the charging facility within the GP region (lines 2–5). The service capacity within the TP region is further optimized when and only when the utilizations of all stations within the GP region satisfy Equation (2). On the other hand, when the utilization is less than the lower threshold, it indicates that the station has a low workload throughout the day and there is facility redundancy. In this case, the facility configuration is refined by eliminating the charging station (lines 10–14) or reducing the chargers by one unit each iteration (lines 15–18). During the refinement phase, the charging network needs to meet the network accessibility constraint Equation (3) and the forward/backward construction constraints Equations (4) and (5) or Equations (6) and (7). When the adjusted number of chargers is less than y^{min}, it is necessary to judge whether to eliminate the station. If Equation (3) is still satisfied after removing the station, the station is removed; otherwise, it is retained.

5 | NUMERICAL EXPERIMENT

In this section, the effectiveness of the proposed three-step planning method is validated on the Nguyen–Dupius network.

As shown in Figure 5, the network consists of 13 road nodes (circles) and four candidate service areas (triangles).

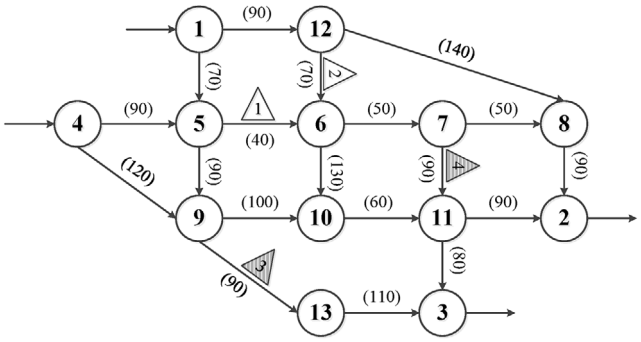

FIGURE 5 The Nguyen–Dupius network with four service areas.

The length of the road is indicated by the number in parentheses. The capacity of the road and the vehicle velocity are set as 2300 pcu and 100 km/h. The flow rates for four OD pairs: (1,2), (1,3), (4,2), and (4,3) have been set at 8, 15, 12, and 8 pcu/15 min. Candidate service areas 1 and 2 are located in the TP region, while areas 3 and 4 are located in the GP region. Each service area is built with one charging station with four chargers at the initial iteration. Referring to Zhang et al. (2022), some parameters are set as follows: $\alpha = 34$RMB/h; $\theta = 1$; $\beta^g = 0.488$RMB/km. Based on the actual data survey, some parameters are set as follows: $\beta^f = 1.29$RMB/KWh; $\xi^e = 0.324$g/KWh; $\lambda^{gas} = 27.6$kg/100km; $\lambda^f = 0.9644$kg/KWh; $y^{min} = 4$; $\lambda^g = 0.009$kg/KWh.The other parameters are set as follows: $S^1 = 40\%$; $S^2 = 20\%$; $n = 2$; $\Omega = 1.5$; $S' = 96$; $\psi = 15$ min; $\beta^{g,up} = \beta^{f,up} = 0.6$, $\beta^{g,down} = \beta^{f,down} = 0.15$; $\beta^g = 0.8\beta^f$.

Six cases (different service area locations and EV penetrations) are tested on a personal PC configured with Intel Core i7-8650U 1.90 GHz and 16 GB RAM. The solutions of each case are listed in Table 3. First, the final solution is obtained by the proposed three-step planning method, as shown in the column "solution." For example, [2: 4; 3:7, 4: 4] indicates that charging stations are built in service areas 2, 3, and 4 with 4, 7, and 4 chargers, respectively. The "Iter" column refers to the number of iterations to get the final solution. The single station charger maximum threshold is set equal to the maximum number of chargers for a single station in the final solution. Then, enumerate all deployment schemes. The "Num^1" is the number of all solutions. The "Num^2" is the number of feasible solutions constrained by Equations (2) and (3). The "Num^3" is the number of nondominated solutions based on the three objectives in Equation (1). The "Num^4" is the number of dominated solutions for the final obtained solution. The "Rank" is the ratio of Num^3 + Num^4 to Num^1. Its meaning is the conservative ranking of the obtained solution among all solutions. The "GPU" is the operation time of finding the final solution.

TABLE 3 Solutions in six cases.

Case	Areas	Perc	Solution	Iter	Num[1]	Num[2]	Num[3]	Num[4]	Rank	GPU (s)
1	1, 2, 4	15%	[1: 4; 2:4, 4: 4]	1	8	1	1	0	12.5%	10.0
2	1, 2, 4	20%	[1: 5; 2:4, 4: 6]	4	64	2	2	0	3.1%	38.1
3	1, 2, 4	25%	[1: 5; 2:4, 4: 10]	8	512	39	13	1	2.7%	83.4
4	1, 2, 3, 4	15%	[2: 4; 3:7, 4: 4]	4	625	50	19	0	3.0%	44.9
5	1, 2, 3, 4	20%	[2: 4; 3:9, 4: 4]	6	2401	58	22	0	0.9%	56.0
6	1, 2, 3, 4	25%	[2: 4; 3:12, 4: 6]	9	10000	275	29	0	0.3%	86.6

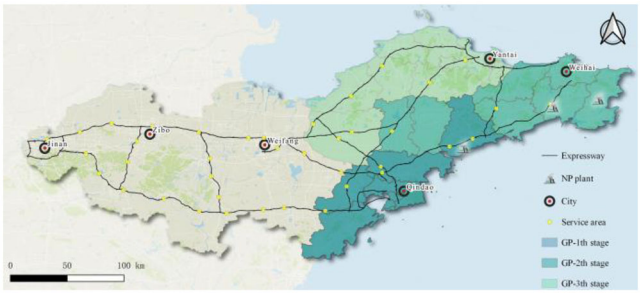

FIGURE 6 Expressway of the Shandong Peninsula.

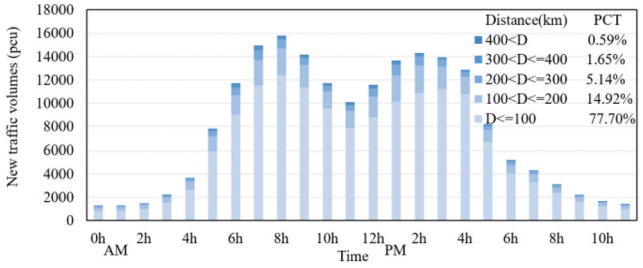

FIGURE 7 Temporal distribution of new traffic volumes at different travel distances.

Analyzing Table 3, some of the conclusions are as follows: (i) With the combined effect of facility utilization and network constraints, the model greatly reduces the size of the feasible solution. In cases 2–6, the percentage of feasible solutions is only 2.4%–8.0% of the total solutions. (ii) Although the method is difficult to obtain all optimal solutions, it can obtain a high-quality feasible solution or even an optimal solution. In cases 2–6, the obtained solutions are ranked in the top 3.1%. (iii) The method efficiently solves the proposed multiobjective problem using the iterative planning method. As shown in Table 3, the number of all solutions increases extremely rapidly as the number of alternative points and EV penetrations increases. The number of iterations is less than 1% of all solutions in cases 2–6. The high solving efficiency is critical in large-scale planning scenarios. We will further discuss the efficiency of the proposed refinement strategy in realistic planning scenarios in Section 6.2.2.

6 | AN EMPIRICAL STUDY

The Shandong Peninsula urban agglomeration is selected as an empirical study. A brief description of the expressway and GP development plan in this case is as follows.

Figure 6 depicts the expressway of the Shandong Peninsula, which connects major cities such as Jinan, Zibo, Qingdao, and Yantai. The network's total length is 2187 km, containing 169 toll stations, 177 roads, and 39 service areas. Referring to the current configuration of constructed charging stations on China's expressways, the EFCS deployment at the initial iteration is set to build one charging station with four chargers in all service areas.

The all-day traffic flow on the network is 188,843 vehicles, with a collection interval of 15 min. Figure 7 presents the temporal distribution of traffic volumes at different travel distances. Intercity travel is mainly concentrated within short distances, with 77.70% of travel within 100 km. Only 7.38% of travel is over distances greater than 200 km, indicating that the proportion of vehicles requiring energy replenishment on the expressway is low.

Currently, the Shandong Peninsula is building a nuclear power cluster to promote the development of nonfossil energy on a large-scale and high proportion. In 2021, Shandong's annual PG was 580.8 billion kWh, of which 521.7 billion kWh is supplied by TP, accounting for 90% of the total. Therefore, Shandong province plans to build a 10-megawatt nuclear power base in the Jiaodong Peninsula to reduce the proportion of TP generation. Nuclear power emits only 5.7 g of carbon per kWh of electricity produced, much less than coal, which emits 357 g. According to the plan, by 2025, the installed nuclear power capacity in operation and under construction will reach about 13 million kW. It will gradually realize the nuclear power supply in the Jiaodong Peninsula.

In this study, five planning scenarios for every 5 years from 2025 to 2045 are set up considering the increases in

TABLE 4 The variables set for 2025–2045 scenarios.

Sequence	Scenario	Year	The growth rate of car ownership	Electric vehicle (EV) percentage	Battery effective capacity	Num[1]	Num[2] (thousand)	Num[3]	GPU (min)
↑	1	2025	–	10%	(0.95, 0.1, 1.0, 0.7)	7	18.88	3	28.6
	2	2030	7%	20%	(0.90, 0.1, 1.0, 0.7)	10	52.97	4	30.4
	3	2035	5%	30%	(0.85, 0.1, 1.0, 0.7)	17	101.41	7	34.8
	4	2040	3%	40%	(0.80, 0.1, 1.0, 0.7)	17	156.75	10	39.5
	5	2045	2%	50%	(0.80, 0.1, 1.0, 0.7)	17	216.33	22	45.8

Note: Num[1]: the number of GP service areas; Num[2]: the number of EV; Num[3]: the number of iterations; GPU: the operation time of single iteration.

car ownership and EV percentage, the battery degradation, and the expansion of GP coverage, as shown in Table 4. Among them, the growth rate of car ownership is predicted based on the change in private vehicle growth rate in Shandong Province in the past 10 years. According to the EV market's development plan and the principle of "moderate advancement" of infrastructure, the percentage of EVs is set to 10%, 20%, 30%, 40%, and 50%, respectively. The battery degradation of the EV group shows a trend of decreasing first and then maintaining stability, and the parameter setting is referred to Wang, Zhao, et al. (2021). According to the development planning of Shandong nuclear power, the GP coverage is set to three stages. As shown in Figure 6, the number of service areas covered by GP is 7, 10, and 17, respectively. The parameters are set as same as those in Section 5. Based on the scenario setup described above, the number of variables involved in the proposed model is huge. Assuming that the maximum charger threshold is 20, the number of decision variables for charging stations is $39 \times (20-4) \times 5 = 3,120$. It is estimated that there are about $\text{sum}(\text{Num}^2) = 546.35$ thousand EV decision variables. The number of facility utilization constraint, network accessibility constraint, and backward construction constraints are $39 \times 5 = 195$, $169 \times 168 \times 5 = 141,960$, and $39 \times 5 \times 2 = 390$. Due to the large size of the network and the heavy traffic flow, the solution time for a single deployment scheme ranges from 28.6 min to 45.8 min. In such large-scale planning scenarios, even heuristic algorithms have difficulty in obtaining a satisfactory solution in an acceptable time.

6.1 | The deployment scheme of charging infrastructures

In this section, using scenario 5 as an example, the iterative optimization process is presented to verify the proposed refinement strategy's effectiveness. The necessity of integrating operation and planning is illustrated. Further, the demand-inducing effects are explored.

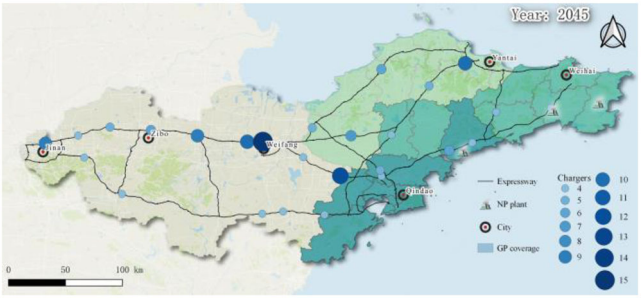

FIGURE 8 Final deployment in scenario 5.

6.1.1 | The final deployment

In scenario 5, the final solution is obtained through 22 iterations. As shown in Figure 8, the EFCS network includes 26 charging stations equipped with 157 chargers. The TP region has 12 charging stations with 78 chargers, and the GP region has 14 charging stations with 79 chargers.

6.1.2 | Working principle and efficiency of the refinement strategy

The working principle and the effectiveness of the proposed refinement strategy in the large-scale planning scenario are demonstrated by analyzing the changes in the network indicators during the iterative procedure, as shown in Figure 9.

In the network's construction scale, the number of charging stations decreased remarkably, and the number of chargers shows a rapid decline and then slow growth. The elimination of inefficient charging stations on the network is basically completed through the first iteration, with 12 charging stations removed. Based on the refinement priority in the proposed refinement strategy, the 2–9 iterations are the optimization process for the charger's configuration in the GP region until the facility utilization meets the threshold condition. Subsequently, the algorithm refines the facility deployment in the TP region. Compared with the current layout, the final EFCS

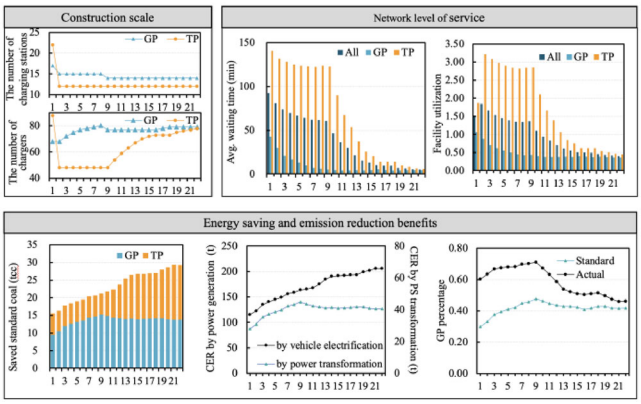

FIGURE 9 The iterative refinement process in scenario 5.

deployment has been significantly optimized, eliminating inefficient stations while improving the service capacity of critical stations.

In network service, the charging network's LOS has been significantly improved, where EVs' average waiting time and facility utilization reach the reasonable range at the final layout. The current layout with the averaged charger allocation leads to a low LOS. The average waiting time is up to 92.52 min, which seriously affects their intercity travel. The GP region's LOS is the first to get a significant improvement in the first eight iterations, where the average waiting time quickly drops from 42.86 min to 6.10 min, and its utilization is improved from 1.06 to 0.43. Improving service capacity in the GP region can relieve some load pressure in the TP region, but providing a high LOS for its charging demand is still challenging. With further facility refinements, the final network LOS reaches a satisfactory level, where the average waiting time is 5.04 min, and the facility utilization is 0.41. On the one hand, the EFCS network with a high LOS plays a great role in safeguarding EVs' intercity travel; on the other hand, it helps achieve sustainable operation of the EFCS full time and protects the operator's return on investment.

In energy and environment, with the refinement of EFCS deployment, the overall ESER benefits gradually increase and stabilize. The GP percentage shows a trend of first increasing and then decreasing. In the first eight iterations, the GP percentage and its ESER benefits have been increasing as the configuration of GP regional facilities is refined. After the eigth iteration, the standard and actual GP percentages reach 48% and 71%, respectively, where its daily GP generation is equivalent to saving 15.72t of SC and reducing 44.68t of CO_2. Further, the overall ESER benefits of the network continue to increase as the service capacity in the TP region improves. In contrast, the benefits brought by GP inevitably decline to some extent. Compared with the current layout, the SC saved by vehicle electrification and its CER under the final EFCS deployment increased by 88.4% (15.5 t–29.2 t) and 78.5% (115.1t–205.5t). Meanwhile, PS transformation also made a significant contribution, with its standardized percentage rising by 12.0% (30%–42%) and CER rising by 44.6% (27.85 t–40.27 t).

In general, the deployment of the EFCS network has been significantly refined by eliminating inefficient stations and improving the service capacity of critical stations. It improves the LOS and ESER benefits of the network significantly, guarantees EVs' intercity travel and the sustainable operation of the facilities, and contributes to the low-carbon development of the expressway.

6.1.3 | The necessity of simulating charging service process

This section explains the necessity of simulation modeling of charging station operation in the CFD. The following three cases model the charging station's service process differently.

1. **NQ case**: The queuing process of EVs at stations is not considered (called no queuing [NQ] case).
2. **QT case**: The second one is the queue theory (QT) case, in which the charging station is modeled as a mathematical queuing system. The waiting time is calculated by $t_{w_{c_i}} = t^0_{w_{c_i}} \cdot [1 + \frac{u_{c_i}}{C_{c_i}} + \frac{{u_{c_i}}^2}{{C_{c_i}}^2}]$, where $t^0_{w_{c_i}}$ is the waiting time of free flow, and this preset parameter is selected for three levels: 2 min, 5 min, and 10 min. u_{c_i} is the number of EVs in the station. C_{c_i} is the service capacity of the charging station, assuming that one charger can serve two EVs per hour.
3. **MS case**: EVs' discrete arrivals and differentiated charging demand in charging stations are considered by the proposed multiagent simulation approach (called MS case).

The three cases are brought into the proposed three-step planning model to obtain the actual operating status of the final layout in each case, as shown in Table 5. The analysis shows that the charging service model has a significant impact on the deployment and operation of the EFCS.

Excessive u_{c_i}-values lead to redundant charging facilities, resulting in lower utilization. Compared with the MS case, the excessive u_{c_i} setting in the QT-10 min case increases the number of chargers to 197, with a 25.5% increase. However, the improvement in environmental benefits from the higher configuration is negligible, with only a 2.8% increase in the total CER. And, the facility utilization decreases 31.7%.

Low u_{c_i}-values or neglected queuing leads to an overload of the facility in actual operation, making it challenging to

TABLE 5 Deployment comparison among three cases.

	No queuing (NQ) case	Queue theory (QT) case			Multiagent simulation (MS) case
		2 min	5 min	10 min	
Construction scale					
Num[1]	26	26	26	26	26
Num[2]	125 (−20.4%)	132 (−15.9%)	161 (2.5%)	197 (25.5%)	157
Level of service					
Time	21.38 (324.2%)	14.27 (183.1%)	4.54 (−9.9%)	1.58 (−68.7%)	5.04
Uti	0.83 (102.4%)	0.66 (61.0%)	0.39 (−4.9%)	0.28 (−31.7%)	0.41
Environmental benefit					
CER	180.31 (−12.3%)	189.49 (−7.8%)	206.95 (0.7%)	211.23 (2.8%)	205.52

Note: Num[1]: the number of stations; Num[2]: the number of chargers; Time: the average waiting time (min); Uti: the facility utilization; CER: the total CER(t).

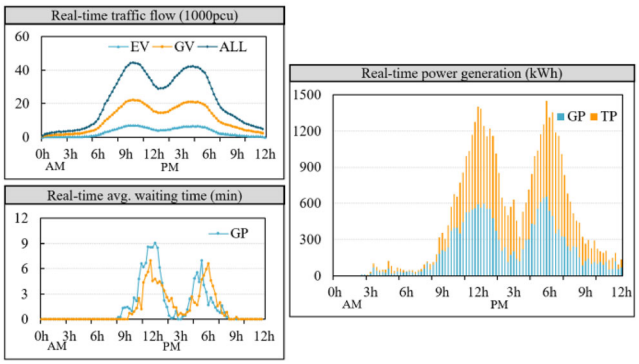

FIGURE 10 The real-time network status.

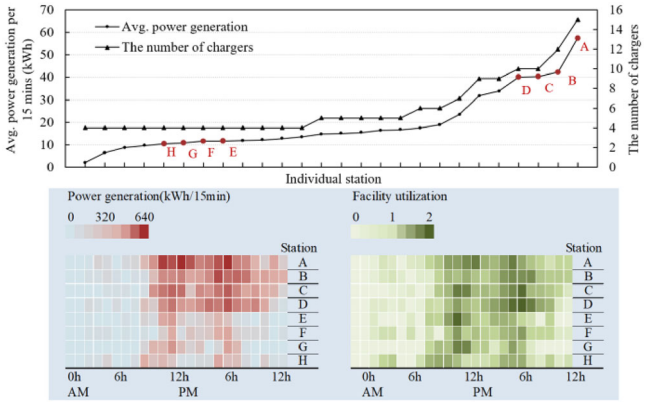

FIGURE 11 The supply–demand matching relationship and real-time operation condition for single station.

maintain sustainable operation throughout the day. Here is an EFCS network with a low LOS in the QT-2 min and NQ cases. The average waiting time in NQ and QT-2 min cases reach 21.28 min and 14.27 min, an increase of 324.2% and 183.1%, respectively. The corresponding facility utilizations reach 0.83 and 0.66, indicating that charging facilities have been under a high load for a long time. Meanwhile, the declined deployment leads to a significant reduction in CER, with a decrease of 12.3% and 7.8%, respectively.

6.1.4 | Network real-time operation

Further, through the analysis of the real-time charging load and facility operation status at the network and the single station levels, the significance of the proposed planning method in integrating operation and planning to ensure the facility's sustainable operation is illustrated.

Figure 10 shows the dynamic changes in traffic flow, the network's LOS, and PG throughout the day. On the expressway, there is an apparent bipeak in traffic flow from 9:00 to 11:00 and 17:00 to 19:00. On the load side, the onset of the bipeak of waiting time and PG in the charging network is delayed backward by about 2 h relative to that of the flow, which is related to EVs' energy consumption characteristics and travel distance. From 9:00 to 20:00, the charging network is at working saturation with slight queues. The charging load in the GP region reaches its maximum at 12:15–12:30, when the average waiting time is 9.02 min, and the PG is 877.66 kWh.

Next, the supply–demand matching relationship for the single station is analyzed. In Figure 11, the 26 charging stations are sorted by the average energy consumption per 15 min. Their service capacities are also displayed. The main results include the following: (i) The load between the charging stations spans significantly, with PG ranging from 1.979 kWh to 57.36 kWh /15 min. Approximately 70% of the stations' PG is concentrated in the 6 kWh–20 kWh /15 min range. (ii) The service capacity of each station has a significant positive correlation with its load. Depending on the size of the charging load, each station is configured with different numbers of chargers, from 4 to 15.

Further, four stations, A, B, C, and D, with higher average PG, and four stations, E, F, G, and H as lower, are selected to compare and analyze their operating status. It is observed that (i) stations A, B, C, and D have significantly

higher charging loads than stations E, F, G, and H during 11:00–20:00, but the differences in real-time utilization are slight. (ii) During the peak period, the utilization of all stations remains in the range [1, 2] most of the time, with the characteristics of "high saturation and low queuing." The low-load stations' utilization remains around 1 during the peak hours, indicating that most of the chargers are in working status, guaranteeing the stations' economy. There are only a few hours for the high-load stations when the utilization is close to 2. Each charger currently has at most one EV in the queue, which guarantees the stations' LOS.

In conclusion, the proposed three-step planning method realizes the integration of operation and planning. The functions of real-time monitoring and evaluating of the charging network's load and operation status at the operation level and the deployment optimization of the facility resources at the planning level are combined by the MA-DTA model. It can effectively allocate facilities according to the dynamic charging load so that each station's real-time LOS and utilization are in a reasonable range and avoid redundancy or shortage of resources.

6.1.5 | Demand inducement effects

The demand-inducing effects of the economic and facility induction methods are explored. In this study, the economic induction method sets different charging prices. There are two methods for facility induction. One sets different deployment refinement priorities. The other sets different LOS. Seven cases are set as follows.

- Case 1: There is no demand-inducing method, that is, TP and GP charging prices are the same, and there i deployment refinement priority is the same in each region.
- Case 2: Set the differentiated charging prices, where $\beta^g = 0.8\beta^f$.
- Case 3: Set the differentiated deployment refinement priorities, as shown in Table 2 (line 2–line 5).
- Cases 4–7: Set differentiated charging prices and deployment refinement priorities. The utilization threshold parameters are the key indicators for determining the charging network's LOS in the proposed refinement strategy. Therefore, using the differentiated LOS method, the value of $\beta^{f,up}$ is set to four levels, which are 0.6, 0.8, 1, and 1.5.

The performance of deployment schemes in various cases is depicted in Figure 12. Comparisons of Cases 1 and 2, and Cases 3 and 4 reveal that the differentiated charging price is less effective in inducing demand in the EFCS network. This is because charging price adjustments have less

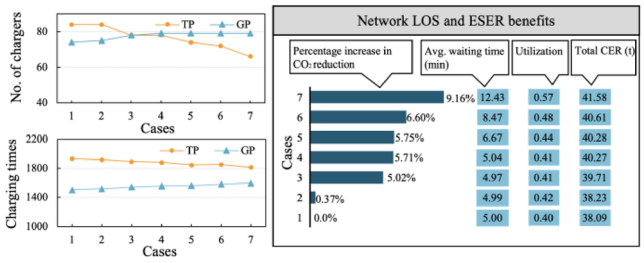

FIGURE 12 Performance of deployment schemes in various cases.

effect on EV users' utility of the charging route. Further, as illustrated in the comparison of Cases 1 and 3, and Cases 2 and 4, the differentiated deployment refinement priority significantly improves the network's ESER benefits by prioritizing the enhancement of the stations' service capacity in the GP region. Take the comparison between Cases 1 and 3 as an example. Implementing the refinement priority strategy increases the service capacity in the GP region, with a corresponding 5.02% increase in the network's CER.

The increase in $\beta^{f,up}$ leads to an imbalance in facilities' LOS in different regions, affecting EV users' charging choices and the network's ESER benefits. As $\beta^{f,up}$ increases from 0.6 to 1.5, the difference in the number of chargers within the TP and GP regions gradually increases from 1 to 13. This causes the total CER of the network to be improved by 3.45%. Meanwhile, the increase of $\beta^{f,up}$ will inevitably cause the network's LOS to decrease. The average waiting time increases from 5.04 to 12.43 min when $\beta^{f,up}$ increases from 0.6 to 1.5. Therefore, planners should coordinate the network's LOS and ESER effects when expecting to induce demand through the differentiated LOS method.

6.2 | Dynamic deployment schemes of charging infrastructures

According to the five scenarios presented in Table 4, the dynamic change of EFCS deployments and network indicators in 2025–2045 are explored as a baseline case.

6.2.1 | Dynamic deployment schemes

Figure 13 shows the obtained dynamic deployment schemes, and the main conclusions are as follows.

1. At the initial stage (scenarios 1 and 2), charging stations will be built mainly on the central road between major cities to maximize stations' service coverage.

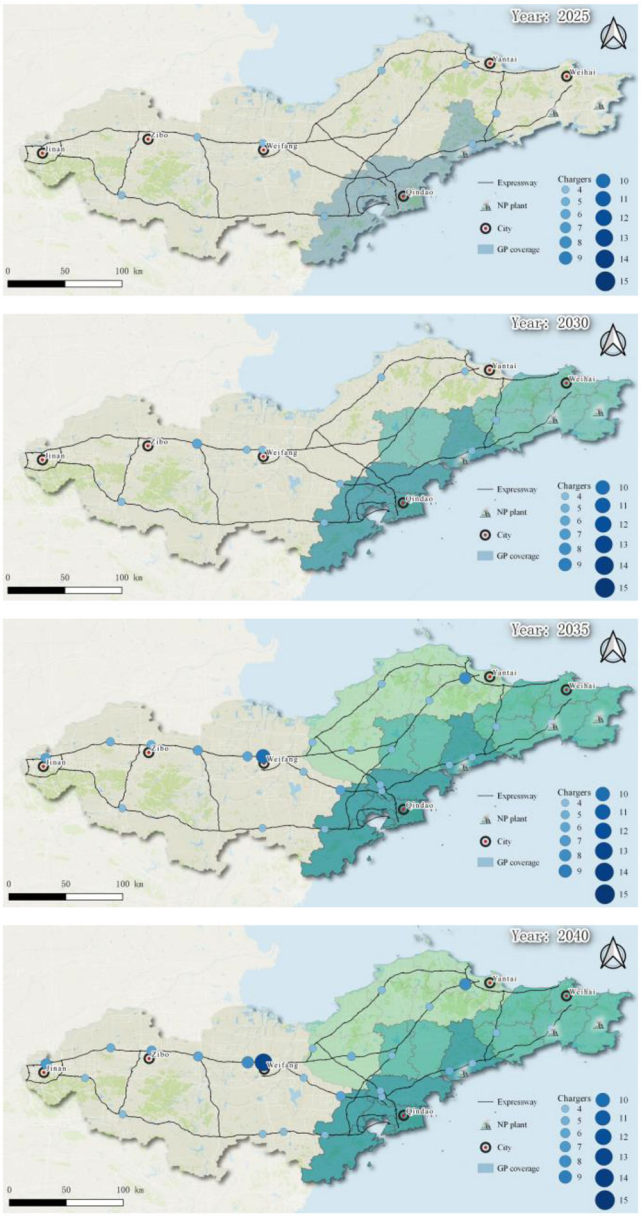

FIGURE 13 Final deployment schemes in various stages.

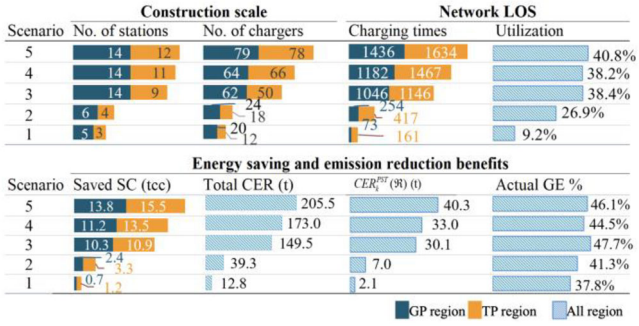

FIGURE 14 Performance of deployment schemes in various stages.

In scenario 1, the eight charging stations configured with the minimum quantity of chargers together compose the fundamental charging network that meets the accessibility of EV intercity travel.

2. Year 2035 is the critical planning period in which the final deployment of the EFCS network in the Shandong Peninsula is basically formed. Between 2030 and 2035, the scale of the EFCS network will expand tremendously: The number of charging stations will increase from 10 to 23, and the number of chargers will increase from 42 to 112. The EFCS layout mostly stays the same in the subsequent development.
3. With the improvement of the EFCS layout, the later planning focuses on service areas around major cities to enhance the service capacity of critical stations. From 2035 to 2045, the number of charging stations increases by only three, while the average number of chargers increases from 4.87 to 6.04 per station. It is observed that charging stations with high configurations are mainly located around major cities, such as Jinan, Weifang, Yantai, and Qingdao. This phenomenon reveals that more land and power supply systems should be reserved to expand charging stations' service capacity in the surrounding service areas of major cities. Meanwhile, according to the traffic flow, economy, and geography, a multifunctional commercial complex–type service area with energy replenishment, shopping, leisure, and entertainment can be created to relieve EV users' time anxiety caused by charging demands.

6.2.2 | Dynamic network indicators

Further, the construction scale, LOS, and ESER benefits variations of the EFCS network in different stages are analyzed, and the statistical results are shown in Figure 14.

Construction scale and LOS

With reasonable deployment planning, the problem of "low utilization" of public charging stations will be solved as the EV market increases. Currently, the "low utilization" phenomenon widely exists in public charging stations, especially on expressways. The low volume of EV intercity travel and the unreasonable EFCS layout cause this phenomenon. With the increase in EV penetration and the orderly construction of the charging network, the EFCS network will serve more EV users, increasing from the initial 234 vehicles per day in 2025 to 3070 vehicles per day in 2045. The facility utilization improves from 0.092 in 2025 to 0.31 in 2030 and stabilizes in a reasonable range 0.38–0.40 during 2035–2045. An appropriate facility utilization guarantees EV users' travel satisfaction and allows the EFCS network to achieve economic sustainability.

TABLE 6 Performance comparison of the NNC and baseline cases.

Scenario	Num[1]	Num[2]	Num[3]	Utl
5	26 (−)	157 (−)	28,392 (−)	40.8% (−)
4	25 (−)	130 (−)	28,392 (−)	38.2% (−)
3	9 (4.3%)	58 (−3.6%)	28,304 (−0.3%)	39.9% (3.8%)
2	6 (40.0%)	26 (−38.1%)	26,212 (−7.7%)	38.7% (44.0%)
1	3 (−62.5%)	12 (−62.5%)	25,132 (−11.5%)	20.1% (117.8%)

Note: Num[1]: the number of stations; Num[2]: the number of chargers; Num[3]: the number of accessible OD pairs for EV; Uti: the facility utilization; CER: the total CER (t).

ESER benefits

In 2035, the ESER benefits derived from the development of the EV market and the PS transformation are greatly enhanced. When the EV percentage increases from 20% to 30%, the full-day SC savings of the network increased from 5.7tcc to 21.1tcc, a 270% increase; and the total CER increased from 39.3t to 149.5t, a 280% increase. Meanwhile, when the entire Jiaodong Peninsula finishes the power transformation, the network's ESER benefits will be greatly enhanced. From 2030 to 2035, the network's actual GP percentage will increase from 23.7% to 47.7%, and the CER by power transformation will increase from 5.6t to 30.1t.

Power transformation is significant in promoting transportation decarbonization. During the expansion of GP coverage from 2025 to 2035, the CER by PS transformation increases from 2.1t to 30.1t. Therefore, different regions should develop various green energy sources such as photovoltaic, wind, geothermal, and nuclear energy according to the local geographical environment, economic development, and energy demand.

6.2.3 | The necessity of network accessibility constraint

In this section, the necessity of network accessibility constraints is demonstrated. A case named NNC (no network accessibility constraint) is set up, which does not consider Equation (3). The performance comparison of the NNC and baseline cases between 2025 and 2045 is listed in Table 6. Figures in parentheses are the percentage change in the indicator in the NNC case compared to that of the baseline case.

The results reveal that the network accessibility constraint's impact on the EFCS network's deployment and operation is mainly in the early stage. In scenarios 4 and 5, the final EFCS deployment in the NNC case is the same as that of the baseline case. Compared to the baseline case, the number of charging stations in the NNC case decreased by 62.5% and 40.0% in 2025 and 2030, respectively. And the facility utilization increased by 117.8% and 44.0%, respectively. It is demonstrated that the EFCS network without network accessibility constraint is more economical in the early stage. However, in 2025 and 2030, 11.5% and 7.7% of the OD pairs are unreachable for EV users in the NNC case. This will limit the coverage of EV trips and reduce the public's willingness to purchase and use EVs.

7 | CONCLUSION

This research aims to provide a practical and reasonable planning method for EFCS's order deployments coordinated with transforming the regional PS. The proposed method is tested in a numerical experiment and applied to an empirical case in the Shandong Peninsula expressway.

The results indicate that the three-step planning method can efficiently get a high-quality solution within acceptable computational time and is applicable to the realistic planning scenario. It is effective in enhancing the EFCS network's ESER benefits by coordinating the charging infrastructure deployment with the uneven PS. Further, the real-time charging load and facility status illustrate that the proposed planning model can effectively allocate facility resources, ensuring each station's dynamic LOS and utilization are reasonable. During the peak period, the station status is "high saturation and low queuing," and the real-time utilization of all stations remains in the range [1, 2]. It demonstrates that integrating the operation and planning realizes the network's sustainable operation full-time, effectively avoiding the heavy congestion at charging stations during peak hours.

In the temporal dimension, backward planning is adopted to explore the multistage deployment schemes under the changing vehicle ownership, EV percentage, battery degradation of EV groups, and PS. The multistage deployment schemes for the Shandong Peninsula urban agglomeration EFCS network from 2025 to 2045 are researched. By observing the changes in the EFCS network, it is found that (1) in the initial stage, the construction focus is expanding stations' service coverage, and the construction object is the central road between major cities; (2) with the increased intercity travel demand

for EVs, the construction focus is shifted to improve the service capacity of critical stations, usually located near major cities. Further, the facility utilization stabilizes from 0.38 to 0.40 between 2035 and 2045, a significant increase compared to 0.095 in 2025. The "low utilization" problem widely existing in the initial stage is solved with the increased EV intercity travel and the mature EFCS network. In ESER benefits, the PS transformation is significant in promoting transportation decarbonization—the network's actual GP percentage increases from 23.7% to 47.7% from 2025 to 2035.

In this research, the planning problem is limited by the simple PS and changes in the external environment. In the future, mixed energy, including photovoltaic, wind, geothermal, and nuclear energy, will be considered in PS. In addition, more comprehensive factors, such as progressive EV mileage and charging technologies, should be considered in the multistage planning.

ACKNOWLEDGMENTS

This work was supported by the National Key R&D Program of China: No. 2023YFB4302703, National Natural Science Foundation of China: 52172312, 71931003, and Singapore Ministry of Education Academic Research Fund (AcRF) Tier 1 project RT22/22.

REFERENCES

Akhand, M. A. H., Ayon, S. I., Shahriyar, S. A., Siddique, N., & Adeli, H. (2020). Discrete spider monkey optimization for travelling salesman problem. *Applied Soft Computing*, *86*, 105887.

Amiri, S. S., Jadid, S., & Saboori, H. (2018). Multi-objective optimum charging management of electric vehicles through battery swapping stations. *Energy*, *165*, 549–562.

An, K., Jing, W., & Kim, I. (2020). Battery-swapping facility planning for electric buses with local charging systems. *International Journal of Sustainable Transportation*, *14*(7), 489–502.

Bao, Z., & Xie, C. (2021). Optimal station locations for en-route charging of electric vehicles in congested intercity networks: A new problem formulation and exact and approximate partitioning algorithms. *Transportation Research Part C: Emerging Technologies*, *133*, 103447.

Bibra, E. M., Connelly, E., Gorner, M., Lowans, C., Paoli, L., Tattini, J., & Teter, J. (2021). *Global EV Outlook 2021: Accelerating ambitions despite the pandemic*. https://trid.trb.org/View/1925380

Bogdanov, D., Gulagi, A., Fasihi, M., & Breyer, C. (2021). Full energy sector transition towards 100% renewable energy supply: Integrating power, heat, transport and industry sectors including desalination. *Applied Energy*, *283*, 116273.

Chen, Z., Liu, W., & Yin, Y. (2017). Deployment of stationary and dynamic charging infrastructure for electric vehicles along traffic corridors. *Transportation Research Part C: Emerging Technologies*, *77*, 185–206.

Ghosh-Dastidar, S., & Adeli, H. (2006). Neural network-wavelet microsimulation model for delay and queue length estimation at freeway work zones. *Journal of Transportation Engineering*, *132*(4), 331–341.

Hajibabai, L., Atik, A., & Mirheli, A. (2023). Joint power distribution and charging network design for electrified mobility with user equilibrium decisions. *Computer-Aided Civil and Infrastructure Engineering*, *38*(3), 307–324.

He, J., Yang, H., Tang, T. Q., & Huang, H. J. (2018). An optimal charging station location model with the consideration of electric vehicle's driving range. *Transportation Research Part C: Emerging Technologies*, *86*, 641–654.

He, S. Y., Kuo, Y. H., & Wu, D. (2016). Incorporating institutional and spatial factors in the selection of the optimal locations of public electric vehicle charging facilities: A case study of Beijing, China. *Transportation Research Part C: Emerging Technologies*, *67*, 131–148.

Hu, D., Zhang, J., & Zhang, Q. (2019). Optimization design of electric vehicle charging stations based on the forecasting data with service balance consideration. *Applied Soft Computing*, *75*, 215–226.

Huang, H., & Savkin, A. V. (2020). A method of optimized deployment of charging stations for drone delivery. *IEEE Transactions on Transportation Electrification*, *6*(2), 510–518.

IEA. (2023), *Global EV outlook 2023*. IEA. https://www.iea.org/reports/global-ev-outlook-2023, License: CC BY 4.0

Ju, Y., Ju, D., Gonzalez, E. D. S., Giannakis, M., & Wang, A. (2019). Study of site selection of electric vehicle charging station based on extended GRP method under picture fuzzy environment. *Computers & Industrial Engineering*, *135*, 1271–1285.

Kang, J., Kong, H., Lin, Z., & Dang, A. (2022). Mapping the dynamics of electric vehicle charging demand within Beijing's spatial structure. *Sustainable Cities and Society*, *76*, 103507.

Kaya, Ö., Alemdar, K. D., & Çodur, M. Y. (2020). A novel two stage approach for electric taxis charging station site selection. *Sustainable Cities and Society*, *62*, 102396.

Li, M., Tang, P., Lin, X., & He, F. (2022). Multistage planning of electric transit charging facilities under build-operate-transfer model. *Transportation Research Part D: Transport and Environment*, *102*, 103118.

Liu, X., Liu, X., Zhang, X., Zhou, Y., Chen, J., & Ma, X. (2023). Optimal location planning of electric bus charging stations with integrated photovoltaic and energy storage system. *Computer-Aided Civil and Infrastructure Engineering*, *38*(11), 1424–1446.

Ma, T. Y., & Xie, S. (2021). Optimal fast charging station locations for electric ridesharing with vehicle-charging station assignment. *Transportation Research Part D: Transport and Environment*, *90*, 102682.

Mas, J. A. (1972). U.S. Patent No. 3,683,256. U.S. Patent and Trademark Office.

Miralinaghi, M., Keskin, B. B., Lou, Y., & Roshandeh, A. M. (2017). Capacitated refueling station location problem with traffic deviations over multiple time periods. *Networks and Spatial Economics*, *17*, 129–151.

Morro-Mello, I., Padilha-Feltrin, A., Melo, J. D., & Calviño, A. (2019). Fast charging stations placement methodology for electric taxis in urban zones. *Energy*, *188*, 116032.

Murnane, M., & Ghazel, A. (2017). A closer look at state of charge (SOC) and state of health (SOH) estimation techniques for batteries. *Analog Devices*, *2*, 426–436.

Pourgholamali, M., Homem de Almeida Correia, G., Tarighati Tabesh, M., Esmaeilzadeh Seilabi, S., Miralinaghi, M., & Labi, S. (2023). Robust design of electric charging infrastructure locations

under travel demand uncertainty and driving range heterogeneity. *Journal of Infrastructure Systems*, *29*(2), 04023016.

Rietmann, N., Hügler, B., & Lieven, T. (2020). Forecasting the trajectory of electric vehicle sales and the consequences for worldwide CO2 emissions. *Journal of Cleaner Production*, *261*, 121038.

Staricco, L., Brovarone, E. V., & Scudellari, J. (2020). Back from the future. A backcasting on autonomous vehicles in the real city. *TeMA-Journal of Land Use, Mobility and Environment*, *13*(2), 209–228.

The People's Republic of China. (2022). 16721 charging piles have been built in expressway service areas across the country. http://www.gov.cn/xinwen/2022-10/31/content_5722812.htm

Uslu, T., & Kaya, O. (2021). Location and capacity decisions for electric bus charging stations considering waiting times. *Transportation Research Part D: Transport and Environment*, *90*, 102645.

Wang, H., Zhao, D., Cai, Y., Meng, Q., & Ong, G. P. (2021). Taxi trajectory data based fast-charging facility planning for urban electric taxi systems. *Applied Energy*, *286*, 116515.

Wang, H., Zhao, D., Meng, Q., Ong, G. P., & Lee, D. H. (2019). A four-step method for electric-vehicle charging facility deployment in a dense city: An empirical study in Singapore. *Transportation Research Part A: Policy and Practice*, *119*, 224–237.

Wang, M., Wang, Y., Chen, L., Yang, Y., & Li, X. (2021). Carbon emission of energy consumption of the electric vehicle development scenario. *Environmental Science and Pollution Research*, *28*, 42401–42413.

Wang, X., Shahidehpour, M., Jiang, C., & Li, Z. (2018). Coordinated planning strategy for electric vehicle charging stations and coupled traffic-electric networks. *IEEE Transactions on Power Systems*, *34*(1), 268–279.

Wei, W., Wu, L., Wang, J., & Mei, S. (2017). Network equilibrium of coupled transportation and power distribution systems. *IEEE Transactions on Smart Grid*, *9*(6), 6764–6779.

Xie, F., & Lin, Z. (2021). Integrated US nationwide corridor charging infrastructure planning for mass electrification of inter-city trips. *Applied Energy*, *298*, 117142.

Yang, J., Dong, J., & Hu, L. (2017). A data-driven optimization-based approach for siting and sizing of electric taxi charging stations. *Transportation Research Part C: Emerging Technologies*, *77*, 462–477.

Yang, W., Liu, W., Chung, C. Y., & Wen, F. (2020). Joint planning of EV fast charging stations and power distribution systems with balanced traffic flow assignment. *IEEE Transactions on Industrial Informatics*, *17*(3), 1795–1809.

Yang, Y., Zhang, T. Y., Zhu, Y. T., & Yao, E. J. (2023). Optimal deploying of charging systems on an expressway network considering the optimal construction time sequence and the charging demand. *Journal of Tsinghua University (Science & Technology)*, *62*(07), 1163–1177+1219. (in Chinese).

Yao, E., & Song, Y. (2013). Study on eco-route planning algorithm and environmental impact assessment. *Journal of Intelligent Transportation Systems*, *17*(1), 42–53.

Zeng, T., Zhang, H., & Moura, S. (2019). Solving overstay and stochasticity in PEV charging station planning with real data. *IEEE Transactions on Industrial Informatics*, *16*(5), 3504–3514.

Zhang, T. Y., Yang, Y., Zhu, Y. T., Yao, E. J., & Wu, K. Q. (2022). Deploying public charging stations for battery electric vehicles on the expressway network based on dynamic charging demand. *IEEE Transactions on Transportation Electrification*, *8*(2), 2531–2548.

Zhang, T. Y., Yao, E. J., Yang, Y., Pan, L., Li, C. P., Li, B., & Zhao, F. (2023). Deployment optimization of battery swapping stations accounting for taxis' dynamic energy demand. *Transportation Research Part D: Transport and Environment*, *116*, 103617.

Zhang, X., Rey, D., & Waller, S. T. (2018). Multitype recharge facility location for electric vehicles. *Computer-Aided Civil and Infrastructure Engineering*, *33*(11), 943–965.

Zhang, Y., Wang, M., Zhang, D., Lu, Z., Bakhshipour, A. E., Liu, M., Jiang, Z., Li, J., & Tan, S. K. (2023). Multi-stage planning of LID-GREI urban drainage systems in response to land-use changes. *Science of the Total Environment*, *859*, 160214.

Zhao, D., Li, X., & Cui, J. (2021). A simulation-based optimization model for infrastructure planning for electric autonomous vehicle sharing. *Computer-Aided Civil and Infrastructure Engineering*, *36*(7), 858–876.

How to cite this article: Zhang, T.-y., Yao, E.-j., Yang, Y., Yang, H.-M., Guo, D.-b., & Wang, D. Z. W. (2024). Multistage charging facility planning on the expressway coordinated with the power structure transformation. *Computer-Aided Civil and Infrastructure Engineering*, 1–23. https://doi.org/10.1111/mice.13216

APPENDIX

Abbreviation		Variables
ESER	Energy saving and emission reduction	$x_{i,k}(\mathfrak{R})$, $y_{i,k}(\mathfrak{R})$: The construction of charging stations and the number of chargers at station i in $\mathfrak{R}$ layout at
EV	Electric vehicle	
EFCS	Expressway fast charging station	X''_k, Y''_k: The optimal deployment of charging stations and chargers at stage k.
TP	Thermal power	$y''_{i,k+1}$: The optimal capacity of the station i in stage $k+1$.
GV	Gasoline vehicle	$H_a^{m,t}$: The energy consumption of vehicle m passing through road a at time t.
GP	Green power	$\overline{v}_{a,t}$: The average speed on road a at time t.
PS	Power structure	$\mathbf{Q}_k(\mathfrak{R})$, $\mathbf{G}_k(\mathfrak{R})$, $\mathbf{U}_k(\mathfrak{R})$: The traffic flow, charging load, and facility utilization in the charging network $\mathfrak{R}$ in stage k.
PG	Power generation	
LOS	Level of service	$Z_k^{\mathrm{tra}}(\mathfrak{R})$: The total travel cost of vehicles in the charging network $\mathfrak{R}$ in stage k.
CFD	Charging facility deployment	$C_{k,m*}(\mathfrak{R})$: The travel cost of m^*.
MCDM	Multicriteria decision making	m^*: $m^* = {}^{m}_{o,d,t,l}$, referring to the vehicle of type m that
MA-DTA	Multiagent-based dynamic traffic assignment	departs at time t and chooses path l through (o, d).
DTA	Dynamic traffic assignment	$q_{k,o,d}^{m,t}$: The new flow between (o, d) at time t.
SOC	State of charge	$P_{k,m*}(\mathfrak{R})$: The choosing probability of path l for m^*.
OD	Origin and destination	$H_{c_i}^{e*}$: The charging demand of e^* at station i.
CER	CO_2 emission reduction	$H_{a,t}^{h}$: The energy consumption of GVs on road a at time t.
SC	Standard coal	$t_{wk,c_i}^{e*}(\mathfrak{R})$, $t_{ck,c_i}^{e*}(\mathfrak{R})$: The queuing time and charging time of e^* at station i.
Sets		$M_{o,d,l}^{m}$: The correction term of path l on OD pair (o, d) for the vehicle of type m.
M: The set of vehicle types, $m \in M = \{h, e\}$. g refers to GV, e		$\partial_{a,l}$: The binary variable, where $\partial_{a,l} = 1$ means that road a is part of path l, otherwise $\partial_{a,l} = 0$.
K: The set of planning stages, $k \in K = \{1, 2, \ldots, k^{\max}\}$.		
Z: The set of power types, $z \in Z = \{g, f\}$. g refers to GP, f refers to TP.		$t_{k,c_i,p,t}^{\mathrm{pile}}(\mathfrak{R})$: The working end time of charger p at station i at time t.
O, D, I: The set of origin, destination, and service areas, $o \in$		$S_{k,c_i}^{e*}(\mathfrak{R})$: The SOC of e^* when it arrives at station i.
$L_{o,d}^{shortest}(N)$, $L_{o,d}^{all}(N)$: The sets of shortest routes and all routes between (o, d).		$t_{ak,c_i}^{e*}(\mathfrak{R})$, $t_{lk,c_i}^{e*}(\mathfrak{R})$, $t_{wk,c_i}^{e*}(\mathfrak{R})$, $t_{ck,c_i}^{e*}(\mathfrak{R})$: The time of arrival, departure, waiting, and charging of e^* at station i.
$\mathfrak{R}$, N, E: The charging, the expressway, and the power distribution network.		
$X_k(\mathfrak{R})$, $Y_k(\mathfrak{R})$: The deployment scheme of charging stati chargers in the network $\mathfrak{R}$ in stage k.		$U_{k,i}(\mathfrak{R})$: The average value of status of station i.
		$q_{k,c_i,t}(\mathfrak{R})$: The number of vehicles at station i at time t.
$\mathbf{W}_k^{\mathrm{OD}}$: The OD travel matrix in stage k.		$E_k^{\mathrm{actual,z}}(\mathfrak{R})$, $E_k^{z}(\mathfrak{R})$: The actual PG and all charging demand in the region with power z.
$L_{o,d}^{h}(N)$, $L_{k,o,d}^{e}(N, \mathfrak{R})$: The effective route sets of GVs and EVs between (o, d) on the network (N, $\mathfrak{R}$) in stage k.		$CER_k^{PG}(\mathfrak{R})$, $CER_k^{PST}(\mathfrak{R})$: The CER by vehicle electrification and PS transformation.
$I_k^z(\mathfrak{R})$: The set of charging stations in power z in the netw k.		$ENG_k^z(\mathfrak{R})$: The quantity of SC required to supply the equivalent energy in the region with power z.
Θ: The EV working status, where driving status $\Theta = 1$ and charging status $\Theta = 0$.		
Parameters		$P_k^{\mathrm{actual,g}}(\mathfrak{R})$, $P_k^{\mathrm{sta,g}}(\mathfrak{R})$: The actual and standard GP percentages.

(Continues)

Abbreviation	Variables
l_a, l_l: The lengths of road a, and path l.	Parameters
Ω: The amplification factor in finding the effective route s	γ_{c_i}: The type of power supply for station i.
n: The maximum times of en-route charging.	θ: The discrete coefficient reflecting users' perception difference.
S_k^0: The initial SOC of EV group for intercity travel in stag	$\beta^{z,up}$, $\beta^{z,down}$: The upper and lower bounds of facility utilization in power z.
$S^{\exp}$: The expected SOC of EV charge en-route.	S': The number of time parts.
S^1: The minimum SOC of EV when leaving the expressw	ψ: The upper bounds of EVs' queuing time.
S^2: EV users' tolerance limit of SOC during driving.	ξ^{e}: The SC coefficient of power.
α: The value of time.	λ^{gas}, λ^{f}, λ^g: The carbon emission factors of gasoline, TP, and GP.
μ^g, μ^f, μ^h: The energy prices of GP, TP, and gasoline.	y^{min}: The minimum number of chargers for a single charging station.